Impact assessment on spatial connectivity and simulation of traffic flows under flood-related road network disruptions

Sustainable Cities and Society 135 (2025) 107003

Contents lists available at ScienceDirect

Sustainable Cities and Society

journal homepage: www.elsevier.com/locate/scs

# Impact assessment on spatial connectivity and simulation of traffic flows under flood-related road network disruptions

Amirehsan Charlang Bakhtyari *, Angela Carboni, Francesco Deflorio, Matteo Ferraro, Lorenzo Sica

*DIATI, CARS@POLITO, Politecnico di Torino, Duca degli Abruzzi 24, 10129 Torino, Italy*

A R T I C L E I N F O

Dataset link: Data for GIS-based spatial vulnerability analysis in the area of Alessandria in Italy in case of road network disruption (Original data), Data for the traffic flow simulation in the area of Alessandria in Italy in case of road network disruption (Original data)

*Keywords:*
Vulnerability
Accessibility
Traffic simulation
Road network
Urban flood

A B S T R A C T

Road networks serve as a critical lifeline for ensuring the mobility of people and goods. The increasing frequency and unpredictability of extreme weather events highlight the need for studies to identify potential vulnerabilities of road networks and assess the negative effects of disruptions on traffic flows. This paper investigates the vulnerability of road networks to flood-induced disruptions, emphasising the use of open data and open-source software tools. Two quantitative approaches are proposed and compared: (i) a GIS-based spatial and topological analysis that assesses network vulnerability without incorporating traffic demand, and (ii) mesoscopic traffic simulation with dynamic traffic assignment to evaluate network performance and functionality under disrupted conditions. These methodologies are applied to a case study in Northern Italy, highlighting their different levels of complexity and applicability depending on data availability. The results indicate that while the spatial and topological approach provides a preliminary identification of vulnerabilities, the simulation method offers a detailed understanding of the dynamic traffic flows under degraded conditions, capturing not only changes in travel distance and time but also the effects of congestion.

## 1. Introduction

Road networks play a key role in ensuring daily mobility for people, facilitating the transport of goods, and serving as a lifeline system during disruptions. Beyond supporting the normal operation of a city (Zhao et al., 2022), road networks are also essential for rescuing people (Kim et al., 2023), safeguarding economic values (Pregnolato et al., 2017; Y. Zhang et al., 2024), and repairing or restoring other infrastructure systems. As a basis of transportation infrastructure, road networks are vital for maintaining societal resilience and mobility, underscoring their importance in sustaining modern life (Mattsson & Jenelius, 2015). Road networks face growing challenges from rapid urbanization, climate change, and interconnected infrastructure systems (Markolf et al., 2019; Tang et al., 2025). These challenges are worsened in urban areas by events such as accidents, congestion, and natural disasters (Zhao et al., 2022). Floods, in particular, have an extreme impact on road networks by disrupting mobility, causing extensive infrastructure damage, and delaying recovery efforts. Flooding in road networks can have severe consequences, posing direct risks, such as drowning, vehicle-related fatalities, and physical damage that leads to road closures, unsafe travel conditions, and infrastructure destruction. Indirectly, it hinders the ability of first responders to address emergencies, contributes to traffic delays and increased congestion, raises fuel consumption and emissions, and results in significant economic, social, business, and environmental losses (Pyatkova et al., 2019; Evans et al., 2020; Ding & Wu, 2023; He et al., 2023).

For example, in the Piedmont region of Italy, a destructive flood struck in November 1994. The most intense event occurred on November 6, 1994, causing widespread damage to facilities and infrastructure. The flood resulted in seventy fatalities and severely affected the provinces of Cuneo, Asti, and Alessandria. The heavy rainfall, which began on the evening of November 4 and continued through November 6, exceeded 300 mm in 36 h at several mountain stations affecting several river basins. The flood caused extensive property damage, estimated at >12 billion U.S. dollars. About one-third of this damage was to public works and agriculture, with 150 bridges either collapsing or suffering significant damage (Buzzi et al., 1998; Mandarino et al., 2021a).

As another example, in May 2023, a series of devastating floods struck the Emilia-Romagna region of Italy. The first wave of flooding

* Corresponding author.
*E-mail address:* amirehsan.charlang@polito.it (A. Charlang Bakhtyari).

https://doi.org/10.1016/j.scs.2025.107003
Received 9 April 2025; Received in revised form 18 November 2025; Accepted 18 November 2025
Available online 20 November 2025

occurred on May 2–3, resulting in two fatalities. However, the most severe flooding occurred on May 16–17, causing at least fifteen fatalities and displacing approximately 50,000 people. Over two weeks, the region received rainfall equivalent to seven months' worth, causing the overflow of 23 rivers. This extreme weather triggered 400 landslides, affecting 43 cities and towns. The provisional cost of the damage was estimated at over 10 billion euros. In terms of transportation, the flooding and landslides caused significant damage to infrastructure. Around 3.6 % of the road network in the affected provinces was disrupted, with the most damage occurring on municipal roads (36.2 %), local roads (35.7 %), and private roads (18.5 %) (Brath et al., 2023). The railway network also suffered, with 14 landslides damaging critical lines, including the Bologna–Florence and Faenza–Florence routes. While the Bologna–Florence line was quickly restored, the Faenza–-Florence line experienced prolonged service disruptions. Furthermore, ongoing landslides, triggered by the saturated ground, continued to cause road closures and isolate communities at a regional scale, demonstrating the indirect impacts of the flooding in the days that followed (Cremonini et al., 2024).

Therefore, road networks are vulnerable to flood events. Reliable road networks, appreciated for their safety, cost-effectiveness, travel efficiency, and regularity of service, play a decisive role in maintaining traffic flow. Whether supporting public transport or private travel, preserving this flow is essential for ensuring production, logistics, and business continuity (Pregnolato et al., 2017). Consequently, it is essential to examine these indirect impacts thoroughly to identify and effectively mitigate the vulnerabilities of road networks. Addressing this challenge has become a critical issue in modern transportation development, particularly from the perspective of urban resilience and sustainable development (Zhao et al., 2022; Rajput et al., 2023).

Accordingly, this paper aims to address the research gap concerning the lack of flexible and replicable methodologies for assessing road network vulnerability to flood events, also in contexts of limited data availability. To this end, this study proposes and compares two methodologies that differ in terms of complexity and data requirements. By relying on publicly available online data and open-source tools for geographic analysis and traffic simulation, the methodology quantifies the impacts of flood-induced disruptions on traffic flow. In contrast, in data-scarce contexts, a GIS-based spatial and topological analysis enables a simplified but informative vulnerability screening. The framework has been developed to ensure adaptability to various contexts, making it applicable at a regional scale and suitable for both urban and rural settings. The paper also clarifies which components can be approximated and what types of insights can be expected accordingly. To demonstrate its applicability and effectiveness, both approaches are applied and explained through a case study in northern Italy, specifically the Alessandria province in the Piedmont region.

The paper is structured as follows: Section 2 reviews the literature on the vulnerability of road networks to extreme events, particularly floods, and their impacts on transportation systems. Section 3 outlines the methodology and framework employed in this study. Section 4 presents the results of the case study application along with a discussion of the findings. Finally, Section 5 provides the conclusions and recommendations for future research.

## 2. Literature review

### 2.1. Definition of road network vulnerability

Ensuring the functionality of road networks is an issue widely studied in the literature. Numerous studies have assessed the consequences of extreme events, such as floods, on road networks. The study of road network vulnerability originated twenty years ago when Berdica (2002) introduced the concept, defining it as the susceptibility of road networks to incidents and disruptions that significantly reduce their serviceability.

Since Berdica's work, the concept of road network vulnerability has evolved, yet a universally accepted definition remains elusive. For instance, Taylor et al. (2006) assessed vulnerability through socioeconomic impacts, defining it as the degradation of network accessibility caused by disruptions. Similarly, Mattsson and Jenelius (2015) described road network vulnerability as the potential degradation of the transport system and its subsequent societal impacts. Other perspectives have emerged based on diverse research contexts and applications, giving rise to concepts such as demand vulnerability, topological vulnerability, dynamic vulnerability, and intrinsic vulnerability (Zhao et al., 2022). For example, Balijepalli and Oppong (2014a) and Morelli and Cunha (2019) emphasized that road network vulnerability extends beyond the susceptibility of individual road segments to hazards. Their work highlights the correlation between factors like network structure, traffic patterns, and economic impacts, underscoring the interconnectedness of the system and the far-reaching consequences of disruptions (Mohebbi et al., 2020). Therefore, vulnerability is a relative concept, depending on the specific hazard and the unique characteristics of the road network. It is also dynamic, evolving over time due to infrastructure improvements, land-use changes, and the increasing frequency or intensity of extreme events. Assessing vulnerability requires a comprehensive approach that accounts for physical, operational, and social factors.

Depending on the availability of input data, researchers adopt various methodologies and indices to assess road network vulnerability. These approaches range from short-term evaluations, which focus on direct and tangible impacts (e.g., physical damage), to long-term assessments of indirect and intangible consequences (e.g., congestion) (M. Taylor, 2017; Rebally et al., 2021; Markolf et al., 2019). Such analyses are crucial for formulating strategies to reduce the vulnerability of road transportation systems to future disruptions. Detecting vulnerabilities is a cornerstone of resilience design in transport systems (Mattsson & Jenelius, 2015; Serdar et al., 2022). Resilience is a system's capacity to adapt when exposed to adverse situations, avoiding potential losses. In transportation, it is usually described as the capacity to recover service levels in a timely manner (Westrum, 2006; Ganin et al., 2017; Y. Zhang et al., 2024; Bi et al., 2025). Therefore, vulnerability is part of the assessment of the resilience of a road network, since it indicates a system's susceptibility to damage from external factors. Resilience assessment additionally includes the quantification of the ability to adapt and recover while maintaining core functions. The weakest links in a network typically require the most attention and timely action to mitigate the magnitude of crises and reduce recovery time. Therefore, a robust preliminary estimate of vulnerabilities is indispensable. Vulnerability analysis is inherently diverse, as different types of crises impact networks in varying ways (Morelli & Cunha, 2019). The following section provides a review of methods employed in research to assess road network vulnerability.

### 2.2. Assessment models of road network vulnerability

Current approaches for assessing road network vulnerability can be broadly categorized into topological and performance-based methods. The former primarily focuses on analyzing changes in the connectivity of the network, while the latter evaluates network performance, including accessibility, serviceability, travel costs, link flow, and capacity (M. Taylor, 2017; Mattsson & Jenelius, 2015; Zhao et al., 2022).

#### 2.2.1. Topologically based methods

Topologically based methods study the structural and interconnective properties of a road network to identify critical nodes (intersections) and links (bridges), whose failure would have the most significant impact (M. Taylor, 2017). These methods mainly analyze the degree of change in road network connectivity before and after a road link failure through graph theory and complex network knowledge, usually including basic topological network connectivity indicators such

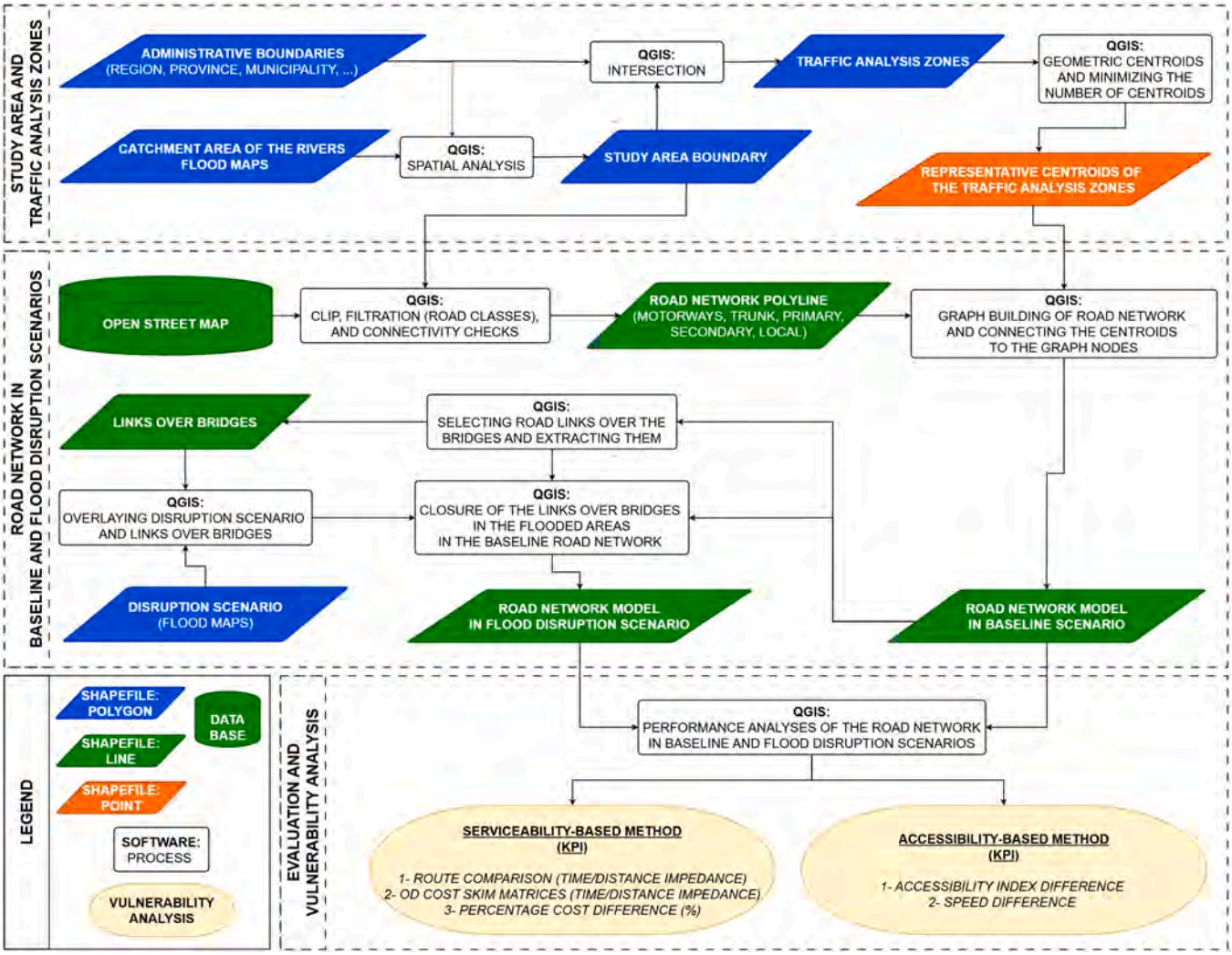


**Fig. 1.** Spatial and topological vulnerability analysis.

as node type, network density, degree distribution, cyclomatic number, parallel path number, and geodesic distance (Zhao et al., 2022). An advantage of this method is its reliance only on topological network data, allowing for scenario comparisons, rapid assessment, and cross-comparison of different networks without requiring detailed link attributes or traffic flow data (Mattsson & Jenelius, 2015; X. Zhang et al., 2015; Gao et al., 2019).

Despite their utility in identifying structural weaknesses, topological methods alone are often insufficient for comprehensive road network vulnerability analysis and planning (M. Taylor, 2017). These methods often neglect critical factors such as the physical attributes of network components, their susceptibility to natural or man-made hazards, and the dynamic nature of traffic flows. Furthermore, static topological analyses fail to capture the evolving interactions within transportation systems and the critical regime shifts that occur during disruptions (Li et al., 2024). To overcome these limitations, topological approaches must be integrated with dynamic modeling techniques and spatial analysis. Broader methodologies often fall into two main categories: accessibility analysis and serviceability analysis, which are discussed in Sections 2.2.2 and 2.2.3, respectively.

### 2.2.2. *Accessibility-Based methods*

Accessibility is a core concept in the transportation sector, conceptualized in multiple ways within the literature, ranging from Hansen's (1959) classic notion of "the potential of opportunities for interaction" to more recent interpretations that emphasize the extent to which land-use and transport systems allow individuals or groups to reach desired activities or destinations through one or more modes of transport (Geurs & Van Wee, 2004; Curl et al., 2015). More broadly, accessibility is the ability to reach valuable destinations by overcoming a generalized cost derived from the friction of moving in space and time (Zhou et al., 2025). Various approaches exist for measuring accessibility, often relying on metrics such as travel time, distance, and network connectivity indices. One of the simplest methods estimates the time required to reach essential services such as healthcare facilities, schools, employment centers, and supermarkets (Curl et al., 2015).

In the case of vulnerability assessment, accessibility-based methods evaluate the impact of disruptions on the ability of individuals or goods to reach their desired destinations using a specific mode of transport. As urban flooding becomes increasingly severe, particularly within transportation networks, some vehicles may be unable to reach their destinations, even with detours, due to widespread road segment disruptions. The appearance of isolated communities reflects a partial loss of spatial accessibility, indicating a gradual degradation of the network's functional connectivity (He et al., 2023).

Alam et al. (2024) assessed accessibility changes before and after Hurricane Irma in Florida, using a cumulative opportunity measure. The study quantifies accessibility to critical facilities by counting the total number of opportunities accessible within specific travel time thresholds (15 and 30 min). Remote sensing and GIS techniques are employed to

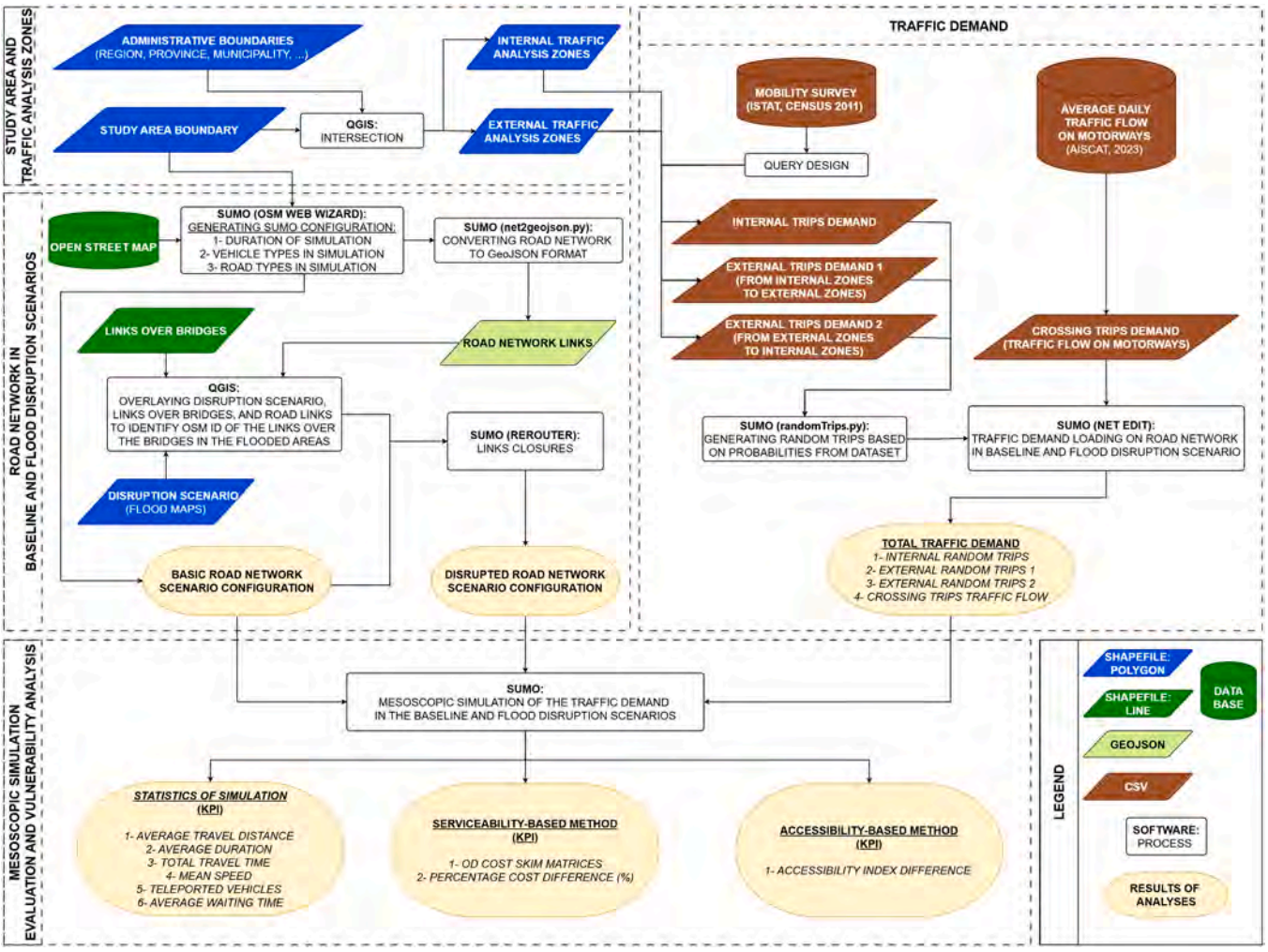


**Fig. 2.** Traffic demand simulation-based vulnerability analysis.

analyze flood-affected areas and measure changes in accessibility at the census block group level. The findings indicate that although several counties in South Florida experienced changes in accessibility to essential facilities, flood exposure does not always directly correlate with vulnerability due to variations in the spatial distribution of these facilities. Similarly, Borowska-Stefańska et al. (2024) evaluated changes in intra-city transport accessibility due to urban flooding. The study employs a distance decay function to model the reduction in interaction potential between origins and destinations as travel time or cost increases. Accessibility changes are measured using modified travel time matrices and weighted comparisons against baseline conditions. The findings highlight significant disruptions in urban connectivity during flood events, with accessibility losses varying based on the spatial distribution of destinations and economic factors such as property values. Martín et al. (2021) assessed road network vulnerability in Valencia (Spain) and Sardinia (Italy) by measuring declines in accessibility due to road closures. The study simulates different road segment removal scenarios (random, criticality-based, and flood-risk-based) and applies a gravity-based accessibility measure to evaluate territorial accessibility changes. Findings suggest that denser networks, like Sardinia's, exhibit greater resilience compared to sparser networks, like Valencia's. The study quantifies accessibility loss through the percentage change in accessibility scores (ACs) relative to baseline conditions.

Building on foundational accessibility metrics, Papilloud and Keiler (2021) refined existing accessibility metrics by incorporating flood-affected populations, opportunities, and average shortest travel time. They developed modified Hansen indices (Hansen, 1959), including the population-weighted Hansen index (A1) and the opportunity-weighted accessibility index (A2). These indices are further enhanced by the transport, opportunity, and population-specific accessibility indices (TOPS-A1 and TOPS-A2), which integrate the impact of flooding on both populations and opportunities while accounting for changes in travel time. The findings highlight the influence of parameter weighting on accessibility assessments and stress the importance of spatial considerations in transportation planning.

In a more behaviorally grounded approach, (Zhou et al., 2025) introduced an activity-based space-time accessibility measure to evaluate the resilience of transit networks under disruption scenarios. Focusing on Xi'an City, China, they modelled how individuals adapt their daily travel and activity schedules in response to transit disruptions of varying severity and duration. Their framework integrated travel behaviors, activity locations, service times, and transit vehicle headways, offering a dynamic and user-centric assessment of accessibility. The study advanced the understanding of transit network resilience by highlighting the interplay between user decisions and system performance during disruptive events.

These studies illustrate the evolution of accessibility-based methods in vulnerability analysis. However, most rely on detailed datasets or computationally intensive models that may not be readily available or applicable across different regional contexts. This highlights a gap for flexible, scalable, and replicable approaches that can accommodate varying levels of data availability while still providing meaningful

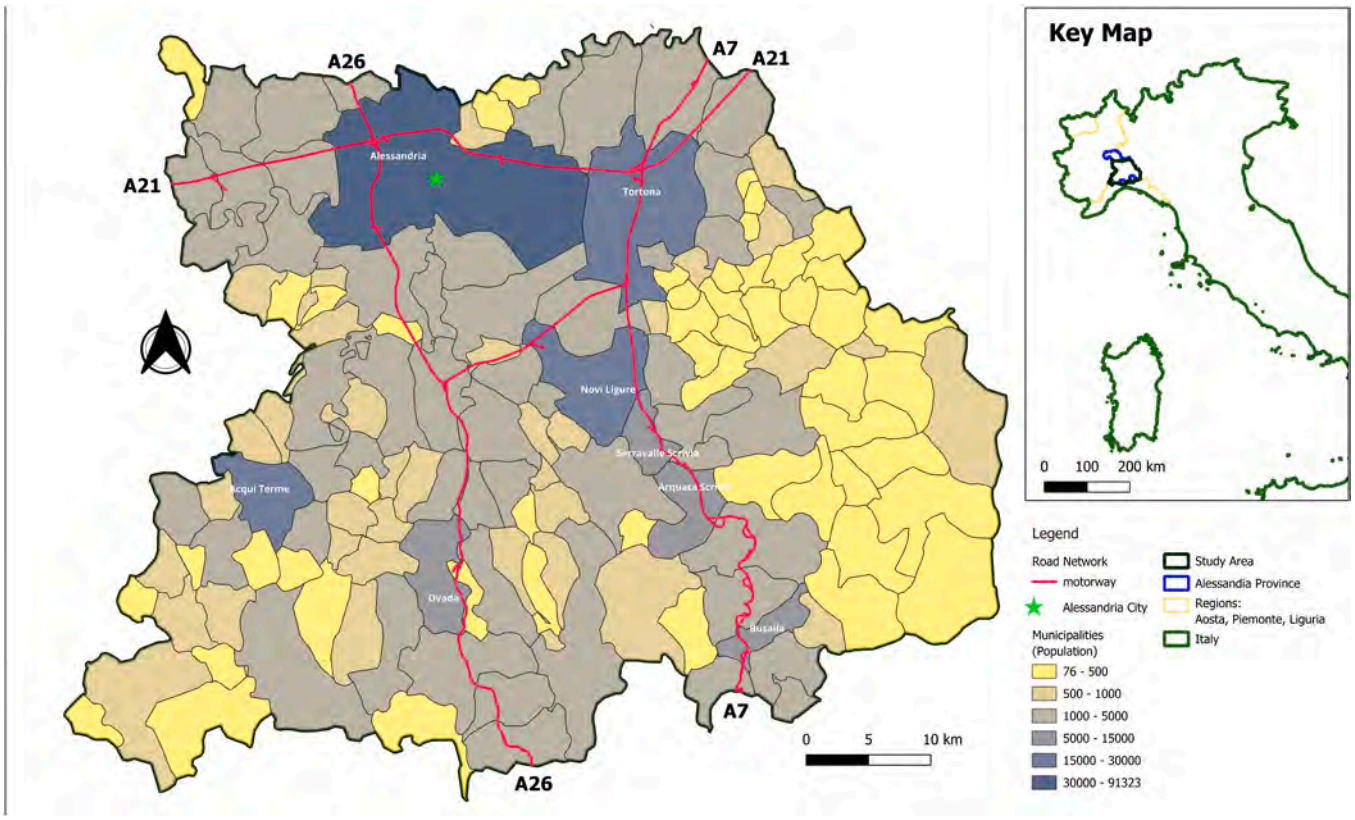


**Fig. 3.** Study area in the southern Piedmont region of northwest Italy.

assessments of accessibility loss due to flood-related disruptions.

*2.2.3. Serviceability-Based methods*

Serviceability-based methods assess the operational performance of road networks under disruption by considering transport-related features such as link and node capacity, link length, travel cost characteristics, and the topological structure of the network. These methods aim to measure the impacts of network failures on traffic operations and travel demand satisfaction (M. Taylor, 2017). The serviceability of a link is defined as its ability to remain usable over a given period, accounting for potential partial degradation. A link is considered critical if its failure significantly impacts network performance. These methods primarily focus on variations in travel costs, including time and distance (Balijepalli & Oppong, 2014). These impedance-based results are typically represented in the form of skim matrices. O-D skim cost matrices quantify the travel cost between each O-D pair. In this study, for example, the impedance values used in the skim cost matrices are based on either travel time or distance. When distance is used as the cost parameter, the resulting paths represent the shortest routes, whereas using travel time yields the fastest paths. This method allows for a basic but informative assessment of network performance, under normal and degraded conditions, in contexts where detailed traffic data are unavailable. In fact, the operational performance of the network can also be quantified using traffic simulation tools if traffic flow data are available. The simulation captures the interaction between traffic demand and network capacity under outage conditions, including capacity and congestion information in the evaluations. Recent research has focused on traffic allocation algorithms to assess network vulnerabilities, particularly regarding levels of service and increased delays due to network disruptions (Morelli & Cunha, 2021). Traffic models simulate how traffic flows through an impaired network with closed or reduced-speed links while satisfying both demand and capacity (Liu et al., 2018; Shahdani et al., 2022). Traffic simulation tools can be categorized into three main groups (Lopez et al., 2018):

- **Macroscopic Simulation**: Models aggregate traffic dynamics, such as traffic density and flow, which are useful for large-scale congestion analysis.
- **Microscopic Simulation**: Simulates individual vehicles and their interactions, offering high precision but requiring significant computational resources.
- **Mesoscopic Simulation**: A hybrid approach that balances large-area representation with greater detail than macroscopic models.

In order to assess road network vulnerability quickly on a regional scale using traffic flow simulation, most studies have relied on macroscopic traffic modeling, which represents congestion and diversion over large areas but lacks the precision of tracking individual vehicles. However, during extreme events such as floods, mesoscopic simulation offers a viable alternative, capturing vehicle movements with greater accuracy while maintaining a manageable computational cost compared to microscopic simulation (Shahdani et al., 2022). They present a framework for assessing the indirect impacts of flooding on road transportation networks through mesoscopic traffic simulation, with a case study focused on Santarém, Portugal. By integrating flood models with traffic simulations in SUMO (Simulation of Urban Mobility) software, the study evaluates traffic disruptions during and after flood events, considering road closures and speed reductions. A key contribution of this research is its comparison of static and dynamic flood integration approaches, where dynamic integration, applying flood maps at different time steps, proves more suitable for capturing the evolving nature of flood impacts, while static integration, using a single flood map, remains practical for post-event disruption analysis. The study highlights the domino effect of flooding, showing that traffic congestion can propagate far from the flooded areas, affecting unexpected parts of the road network.

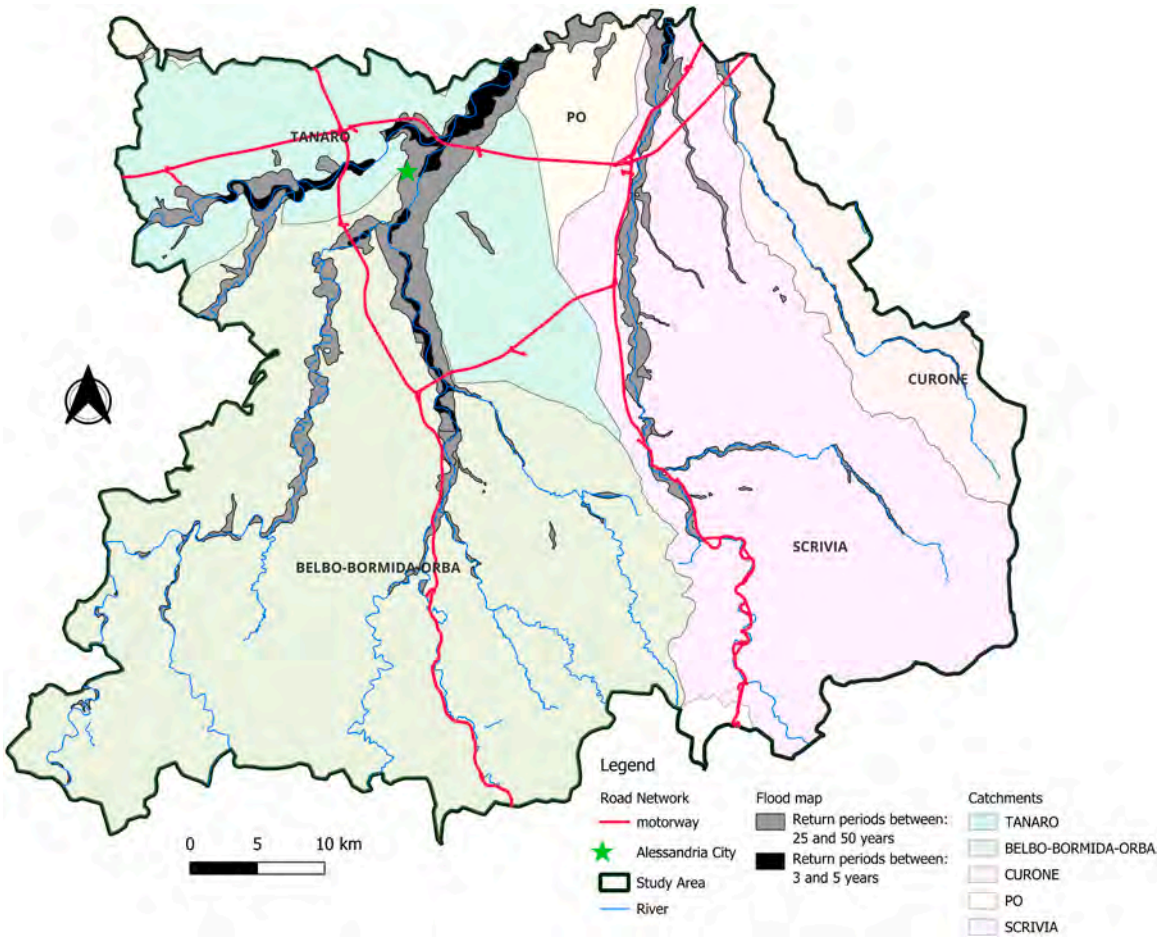


**Fig. 4.** Rivers, catchment areas, and floodplain map in the study area.

For example, Aghababaei et al. (2020, 2021) utilised a mesoscopic simulation approach with traffic simulation software (Aimsun Next ®) to evaluate the operational performance of the South Island of the New Zealand road network following a potential Alpine Fault Magnitude 8 earthquake. Their analysis focused on link closures in traffic simulation, assuming the user's perfect knowledge of disrupted roads. The performance measures, including mean travel time, total travel time, total travelled distance, and flow, were used to conduct both corridor and district trip analyses. The findings indicated that trips that can occur typically face a significant increase in travelled distance and, consequently, travel time. This mesoscopic simulation provided valuable insights into emergency response and transportation organisations, offering a framework for understanding and mitigating the transportation impacts of large-scale extreme events.

## 3. Methodology

The proposed methodology assesses road network vulnerability with the aim of ensuring replicability in other large-scale study areas that have access to similar open and publicly available datasets, as described in Section 1. It combines varying levels of complexity, beginning with preliminary spatial and topological assessments of accessibility and serviceability at key points in the study area using a geographic model in QGIS. The process then advances to a mesoscopic traffic simulation model (Shahdani et al., 2022) in SUMO, enabling the analysis of traffic flow evolution across different sections of the road network. The two methodologies share certain steps such as the definition of the study area (3.1), the road network in both normal and degraded conditions (3.2) and some useful indicators for the final evaluation (3.4). The specific details of the two approaches are instead detailed in Sections 3.5 and 3.6.

### 3.1. Study area and zoning

The first step for both methodologies involves defining the study area, which requires open-access data sources, such as vector shapefiles of administrative boundaries of provinces and municipalities as well as river catchments to account for regional rainfall patterns. Flood hazard maps, indicating flood return periods and the severity of potential flood events, are essential for identifying flood-prone areas and for generating static flood scenarios. These key shapefiles, including administrative boundaries and flood maps, are typically available through official geoportals or online sources, such as OpenStreetMap (OSM).

Once the study area is defined, it is subdivided into traffic analysis zones (TAZs), with centroids representing trip origins and destinations. Administrative boundaries, such as municipalities, along with attributes like name, code, area, and population, serve as the basis for defining these zones. To keep the model manageable and focused on the most representative zones, reducing the number of centroids is advisable, since in the calculation of O-D skim cost matrices, the number of rows and columns would increase significantly with a higher number of centroids. The reduction in centroids directly affects the size of the O-D skim cost matrix, as the number of cells is equal to the square of the number of centroids. Therefore, reducing their number helps maintain analytical tractability, facilitating both post-processing and visualization of accessibility and cost results. Municipalities are initially clustered using the k-means clustering algorithm, with geographic distance as the clustering criterion. This process results in a manageable number of

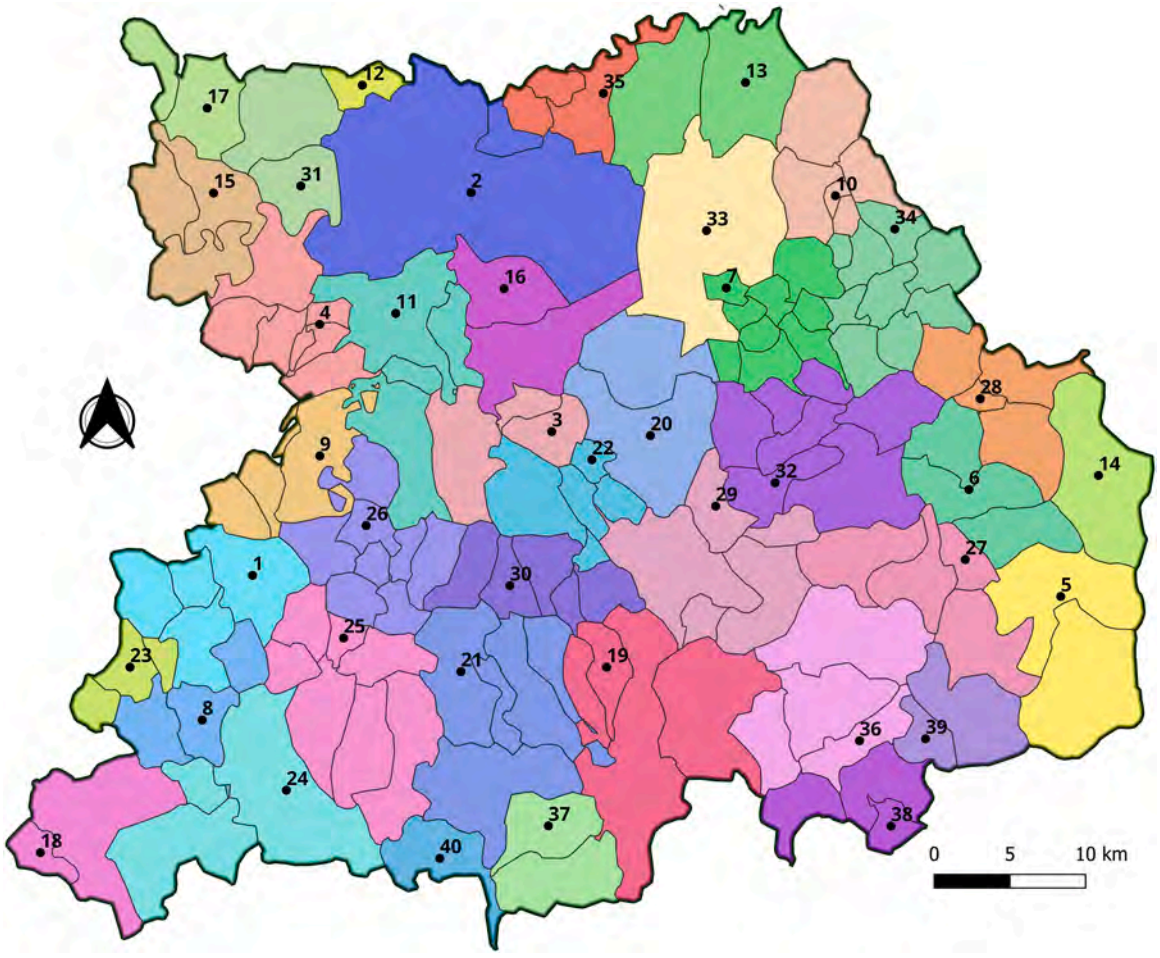


**Fig. 5.** Clustered TAZs and representative centroids.

**Table 1**
Representative centroids within the study area.

| ID | MUNICIPALITY NAME | ID | MUNICIPALITY NAME | ID | MUNICIPALITY NAME | ID | MUNICIPALITY NAME |
|---|---|---|---|---|---|---|---|
| 1 | Acqui Terme | 11 | Castellazzo Bormida | 21 | Ovada | 31 | Solero |
| 2 | Alessandria | 12 | Castelletto Monferrato | 22 | Pasturana | 32 | Stazzano |
| 3 | Basaluzzo | 13 | Castelnuovo Scrivia | 23 | Ponti | 33 | Tortona |
| 4 | Borgoratto Alessandrino | 14 | Fabbrica Curone | 24 | Ponzone | 34 | Volpedo |
| 5 | Cabella Ligure | 15 | Felizzano | 25 | Prasco | 35 | Alluvioni Piovera |
| 6 | Cantalupo Ligure | 16 | Frugarolo | 26 | Rivalta Bormida | 36 | Busalla |
| 7 | Carbonara Scrivia | 17 | Fubine Monferrato | 27 | Rocchetta Ligure | 37 | Campo Ligure |
| 8 | Cartosio | 18 | Merana | 28 | San Sebastiano Curone | 38 | Casella |
| 9 | Cassine | 19 | Mornese | 29 | Serravalle Scrivia | 39 | Crocefieschi |
| 10 | Castellar Guidobono | 20 | Novi Ligure | 30 | Silvano d'Orba | 40 | Tiglieto |

clusters. Within each cluster, the geometric centroid of the municipality with the highest population density is selected as the representative centroid for that cluster. This approach is adopted in the present study to reduce the number of centroids while preserving both spatial distribution and population relevance. The choice, which may affect the final results, is primarily guided by data availability and is intended as a first-cut, preliminary setup to establish a feasible and interpretable analytical framework. Nonetheless, depending on the research objectives and data availability, alternative methods may be used, such as using all centroids for greater spatial granularity or applying other approaches for selecting the centroids of interest.

### 3.2. Road network model

The road network model is developed by selecting relevant road elements from existing transportation infrastructure. A dataset that includes attributes such as road type, classification, length, number of lanes, traffic direction, and speed limit is generally more suitable for streamlining the modelling process. Additional data on tunnels, viaducts, bridges, and critical infrastructure points further support vulnerability assessments in flood scenarios. The road network datasets can be obtained from freely available online data sources, such as OpenStreetMap (OSM).

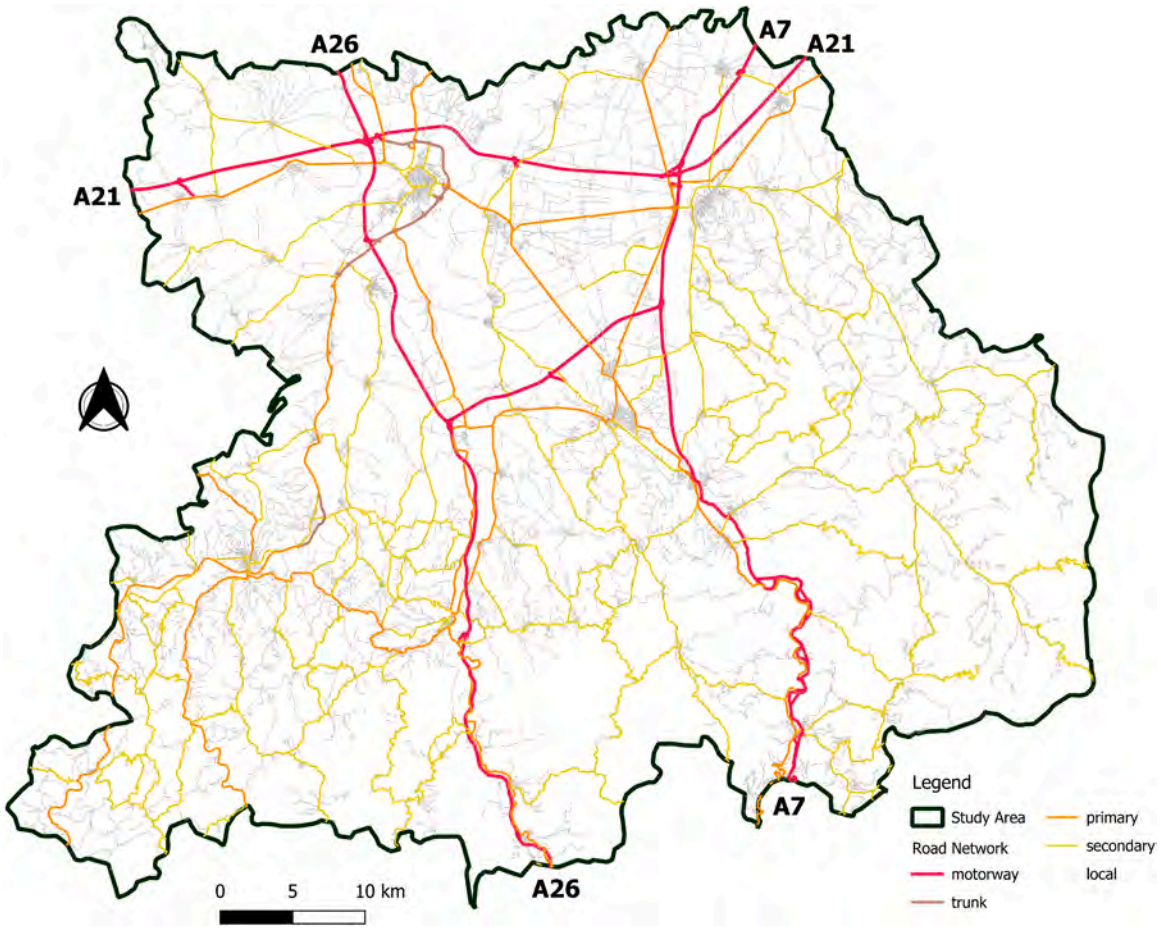


**Fig. 6.** Road network.

### 3.3. Disrupted scenario definition

Disruption scenarios represent a key input for vulnerability assessment and can be defined through different methods, resources and data sources depending on the objective. For instance, by focusing on a predefined list of critical bridges, a specific river basin, or by using flood hazard maps. The objective of this phase of the methodology is to generate a modified (degraded) version of the road network that can be analysed and compared against the baseline (undisrupted) scenario to evaluate the vulnerability of the road networks to flooding events.

One widely used method for generating disruption scenarios is the spatial overlay of flood hazard maps with road network data. Depending on data availability, flood hazard maps can be categorised as either static (representing a specific flood extent) or dynamic (time-varying flood progression). In this study, static flood-disrupted scenarios are developed by identifying bridges within flood-prone areas through overlaying flood maps with a vector shapefile representing road links over bridges. Since bridges are among the most vulnerable links in flood-prone zones, their identification allows for their closure in the simulation, reflecting real-world conditions where they may become inaccessible or unsafe during flood events.

Dynamic flood scenarios, on the other hand, require additional inputs, including rainfall data and a Digital Elevation Model (DEM). Rainfall records simulate precipitation patterns, while the DEM provides terrain elevation for modeling surface runoff and flood inundation. Time-dependent flood maps are needed to capture the spatial and temporal evolution of flooding and its impact on road traffic (Shahdani et al., 2022).

### 3.4. Evaluation and vulnerability indicators

Key indicators such as differences in travel time and distance are calculated to assess the impact of disruptions on the road network. Additionally, comparing average speeds across different scenarios provides insights into how network performance is affected by such disruptions. The effects of disruptions are quantified through two main approaches described in Section 2.2:

- Serviceability-based methods involve route comparisons based on O-D skim cost matrices, which represent impedance in terms of travel time or distance. The percentage cost difference between the disrupted and baseline scenarios is then calculated using Eq. (1).

$$\textit{Percentage Cost Difference}\ (\%) = \frac{C_{ij,disrupted} - C_{ij,\ baseline}}{C_{ij,\ baseline}} * 100 \quad (1)$$

Where $C_{ij}$ represents the cost (either distance or time) of travel between centroids $i$ and $j$.

- Accessibility-based methods rely on accessibility indices to quantify the ease of reaching locations within a transport network. One such index, introduced by Ceccato et al. (2020), evaluates accessibility as the ratio between the minimum distance between the two centroids from the road network and the minimum travel time between the two zones. In this context, travel speed (km/h) is not computed along the minimum travel time route, which can use high-speed options, such as motorways, and overestimates accessibility, without considering the effect of inefficient connections across the network. The study introduces a distinction between two forms of accessibility: active accessibility, which refers to the ease with which a traveller can reach a destination, and passive accessibility, which reflects how easily others can reach a location.

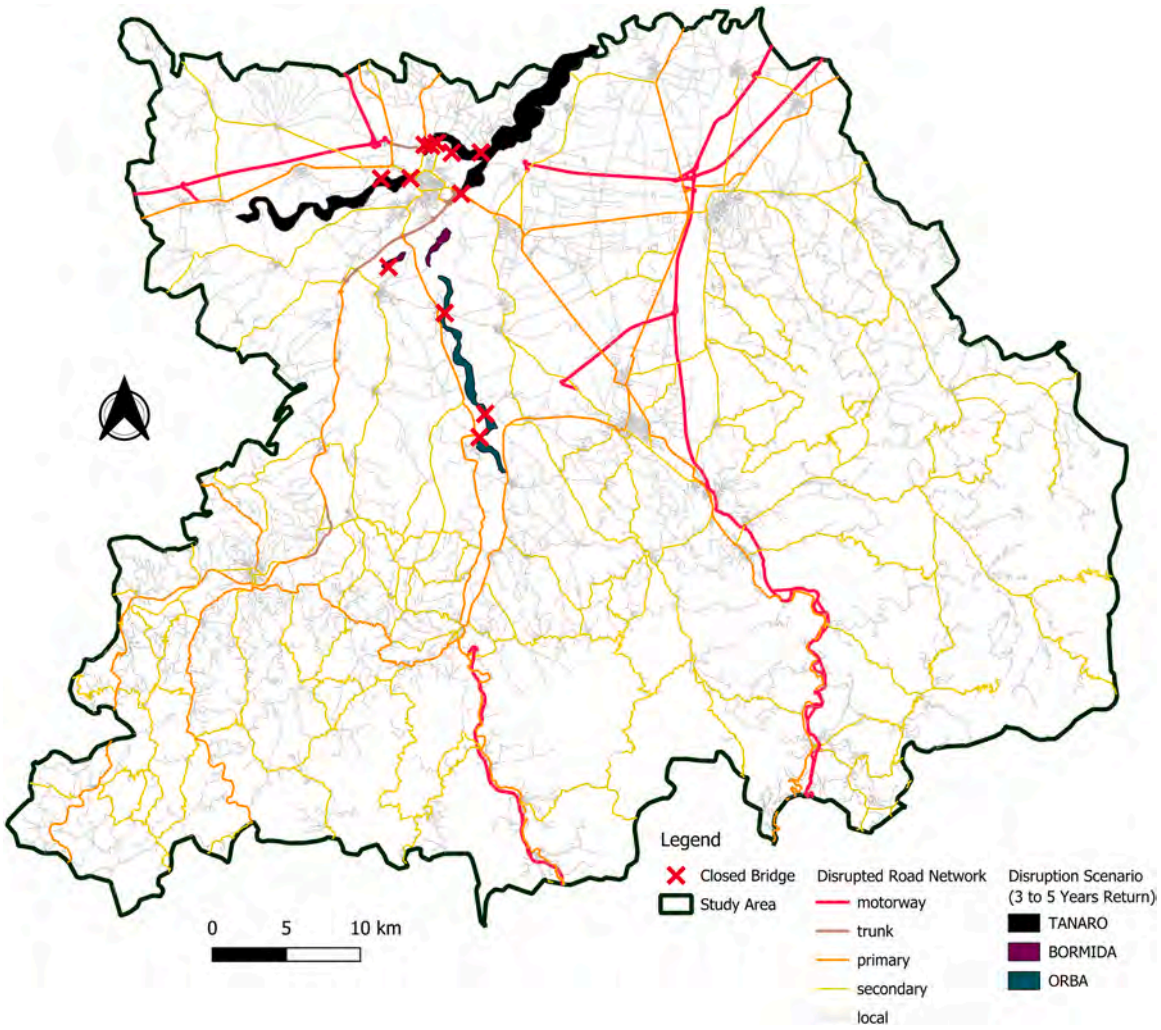


**Fig. 7.** Disrupted scenario, closed bridges, and disrupted road network.

Building on this concept, in this study, the accessibility index (AI) is defined as average speed (km/h), calculated as the ratio between travel distance and travel time along the fastest path between each O-D pair, which is able to capture and compare relationship between zones at any distance.

$$AI_{ij} = dist_{ij}/time_{ij} \tag{2}$$

Where $time_{ij}$ is the minimum travel time between zones $i$ and $j$ and $dist_{ij}$ is the corresponding distance of the selected path.

To assess accessibility changes under flood-induced disruption scenarios, the accessibility index defined in Eq. (2) is adapted by calculating the difference between the disrupted and baseline scenarios. This is expressed in Eq. (3):

$$AI_{ij,difference} = \left(\frac{dist_{ij}}{time_{ij}}\right)_{disreuted} - \left(\frac{dist_{ij}}{time_{ij}}\right)_{baseline} \tag{3}$$

This accessibility index, based on average speed, provides an integrated assessment of the road network's performance by combining both travel time and distance into a single efficiency indicator. Indeed, travel time alone could estimate how long a trip takes but could be compared only among trips of similar length. In contrast, the distance-time ratio allows for consistent comparison of accessibility between O-D pairs with different distances and for assessing the severity of disruptions.

### 3.5. Spatial and topological analysis

Fig. 1 presents a schematic representation of the open data sources and GIS-based tools utilized throughout the methodology for assessing road network vulnerability without incorporating traffic demand. This process primarily relies on QGIS software.

Following the definition of the study area and the selection of a reduced number of representative centroids based on TAZs, the road network layer is downloaded from OSM using the QuickOSM plugin in QGIS. The Topology Checker toolbox is then employed to ensure the connectivity, accuracy, and integrity of the road network data. To convert the spatial network into a format suitable for analysis, the Build Graph tool from the Networks toolbox is used. This tool transforms the physical infrastructure, roads, and intersections into a graph-based model, capturing the topological structure and connectivity of the network, which forms the basis for subsequent analyses. Next, the Build Connectors tool from the Networks toolbox is used to link the representative centroids to the road network. This step establishes connections between the centroid point layer and the nearest nodes of the road graph within a user-defined radius, ensuring that all centroids are properly integrated into the network model.

Once the baseline road network model is established, disruption scenarios are developed to assess vulnerabilities, as outlined in Section 3.3. To simulate flood-related disruptions, flood hazard layers are overlaid with the road network in QGIS. Bridge links located within flood-prone zones are identified and marked for closure. The set of

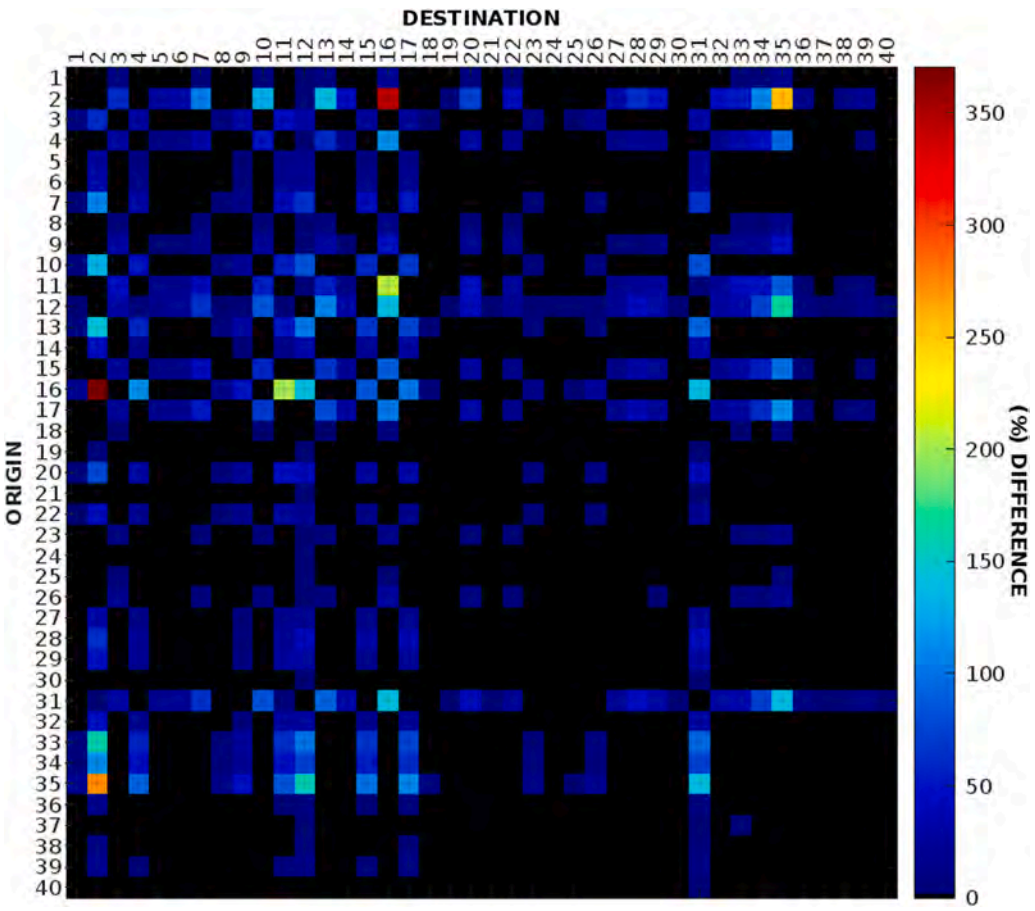


**Fig. 8.** Spatial and topological analysis: O-D percentage cost difference skim matrix, distance impedance.

closed links is then determined by merging the spatial flood data with the vector road network layer. To reflect real-world flood impacts, closures are not limited to individual bridge segments; instead, they are propagated along the connected road segments up to the first entry or exit point of the network. This step is particularly crucial for motorways, where closures are extended to the first interchange, mimicking real-world practices where drivers are informed of closures well in advance to allow for rerouting.

To quantify road network vulnerability using serviceability-based methods, the QNEAT3 toolbox in QGIS is applied to compute O-D skim cost matrices for both baseline and disrupted scenarios. These matrices are calculated using both distance and travel time as impedance factors. The percentage difference in impedance values between the scenarios is then computed to assess the impact of disruptions.

For assessing vulnerability using accessibility-based methods, the Shortest Path tool from the Network Analysis toolbox is utilized to generate fastest path trees (based on travel time) from one selected centroid to all other representative centroids in the study area. For each scenario, baseline and disrupted, the Accessibility Index is computed using the travel time and distance of the generated paths, enabling a comparison of accessibility levels and identifying the impact of flooding on network performance.

### 3.6. Mesoscopic traffic simulation

Fig. 2 illustrates the procedure for evaluating road network vulnerability through mesoscopic traffic demand simulation. Including traffic demand into vulnerability analysis requires spatially detailed trip data, which can be challenging to obtain due to coverage constraints. The dataset should include internal trips within the study area, trips that originate from or are directed to external zones, and trips that pass through the area. In general, travel demand data consists of attributes such as trip origin and destination, purpose, travel time, mode of transportation, and trip duration. To effectively manage demand in the model, traffic demand is disaggregated into the three spatial categories mentioned above.

Starting from the defined study area and TAZs, traffic demand can be derived from two main open data sources. Mobility data from national census surveys could provide insights into internal and external trips, while aggregated traffic flow data from average daily traffic on motorways can help estimate the number of crossing trips within the study area.

Once the demand data is structured, it is assigned to the road network using a mesoscopic traffic simulation approach in SUMO. Mesoscopic simulation offers a balance between data resolution, computational efficiency, and network size. Compared to microscopic simulation, it is significantly faster (up to 100×), more tolerant of modeling errors (especially at intersections and lane-changing areas), and suitable for regional-scale networks.

To simulate external and crossing trips accurately, external zones and key entry and exit points to the study area are defined. These typically include motorway edges and major national roads intersecting the study area boundary. Synthetic traffic demand is generated using SUMO's RandomTrips module and traffic flow definition. A set of trips is generated between randomly selected origin and destination edges within the road network. The probability distribution of trips is aligned with the demand characteristics of each zone. Internal and external trips, queried from census data, are distributed randomly across road edges based on probability weights derived from demand datasets. In contrast, traffic flow on the motorways is directly assigned to the road

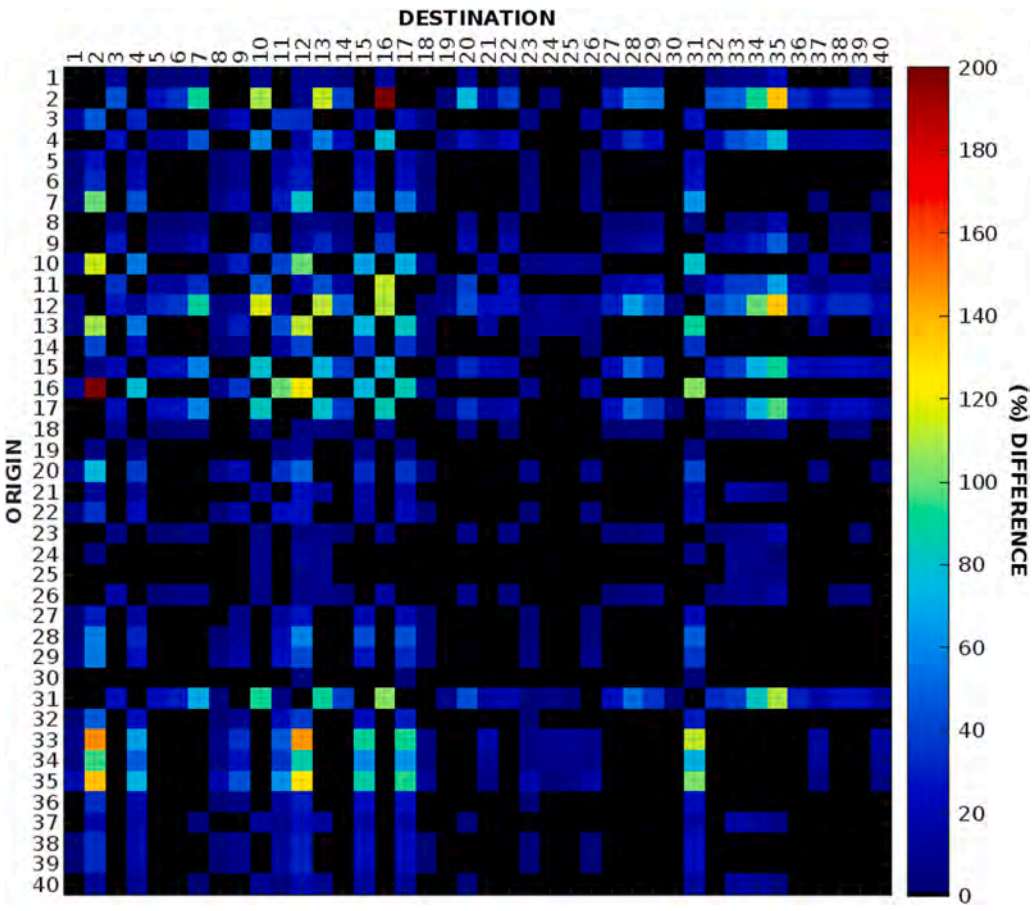


**Fig. 9.** Spatial and topological analysis: O-D percentage cost difference skim matrix, time impedance.

network for crossing trips, as they can be directly connected to road edges at the defined entry and exit points of the study area.

The road network is initially acquired using the OSM Web Wizard, a SUMO-integrated tool that imports road data from OSM based on road classifications, vehicle types, and simulation duration for the desired geographic extent. The SUMO Netedit tool is then used to process the road network data obtained from OSM, generating the final simulation input, which includes vehicle types, characteristics, feasible routes, and departure times.

The flood disruption scenario is integrated by identifying disrupted edges through a GIS-based overlay of the flood hazard map and the road network exported from SUMO using a Python code called "net2geojason.py". This disrupted network is imported into SUMO, and the rerouter function in the SUMO traffic simulator is used to manage temporary or permanent road closures. This function allows specific road links to be closed for certain vehicle types, forcing dynamic route recalculations. The same traffic demand in the baseline scenario is assigned to the disrupted road network to allow a consistent comparison of criticalities and congestion patterns. The mesoscopic traffic simulation enables the observation of congestion effects, such as delays and traffic jams, under the disrupted scenario. Additionally, bridge closures can be configured for specific time intervals in the simulation to assess time-dependent variations in traffic conditions. The impact of the flooding event on the road network is assessed by comparing simulation outcomes between the disrupted and baseline scenarios. The effects on traffic performance are expressed through three key indicators: additional travel time, additional travel distance, and reduction in average speed. To further evaluate the severity of network disruptions, the number of teleported vehicles in the flooded scenarios is analyzed. This metric indicates the extent of congestion, identifying cases where vehicles are either trapped in traffic jams or unable to reach their destinations due to road closures. It serves as a direct measure of the network's reliability and vulnerability. Moreover, the mean waiting time of vehicles is assessed, representing the duration at which vehicle speed remains below or equal to 0.1 m/s, excluding scheduled stops.

Finally, the mesoscopic simulation results, particularly trip-level information, are aggregated at the zonal level, allowing the accessibility index and skim cost matrices to be compared with the findings obtained from the spatial and topological vulnerability analysis. By manipulating the trips information as one of the outputs of the mesoscopic simulation, which contains detailed attributes for each vehicle such as ID, departure and arrival times, departure delays, departure and arrival speeds, trip duration, route length, waiting time, and time loss, it is possible to aggregate trip data at a zonal level and subsequently at a representative centroid level, forming an O-D skim cost matrix that captures both distance (average route length between representative centroids) and time (average travel time between representative centroids) impedance under baseline and disrupted scenarios. The percentage cost difference between the two scenarios is then computed using Eq. (1). By analysing the average trip duration and distance for all trips originating from one selected centroid to all other representative centroids in the study area, the AI difference, representing reduced average speed (km/h), between the baseline and disrupted scenarios, is computed using Eq. (3).

### 3.7. Validation of the mesoscopic simulation

Due to the absence of observed traffic data during flooding events, the mesoscopic traffic simulation model is validated using typical traffic conditions from the baseline scenario. The validation focuses on average

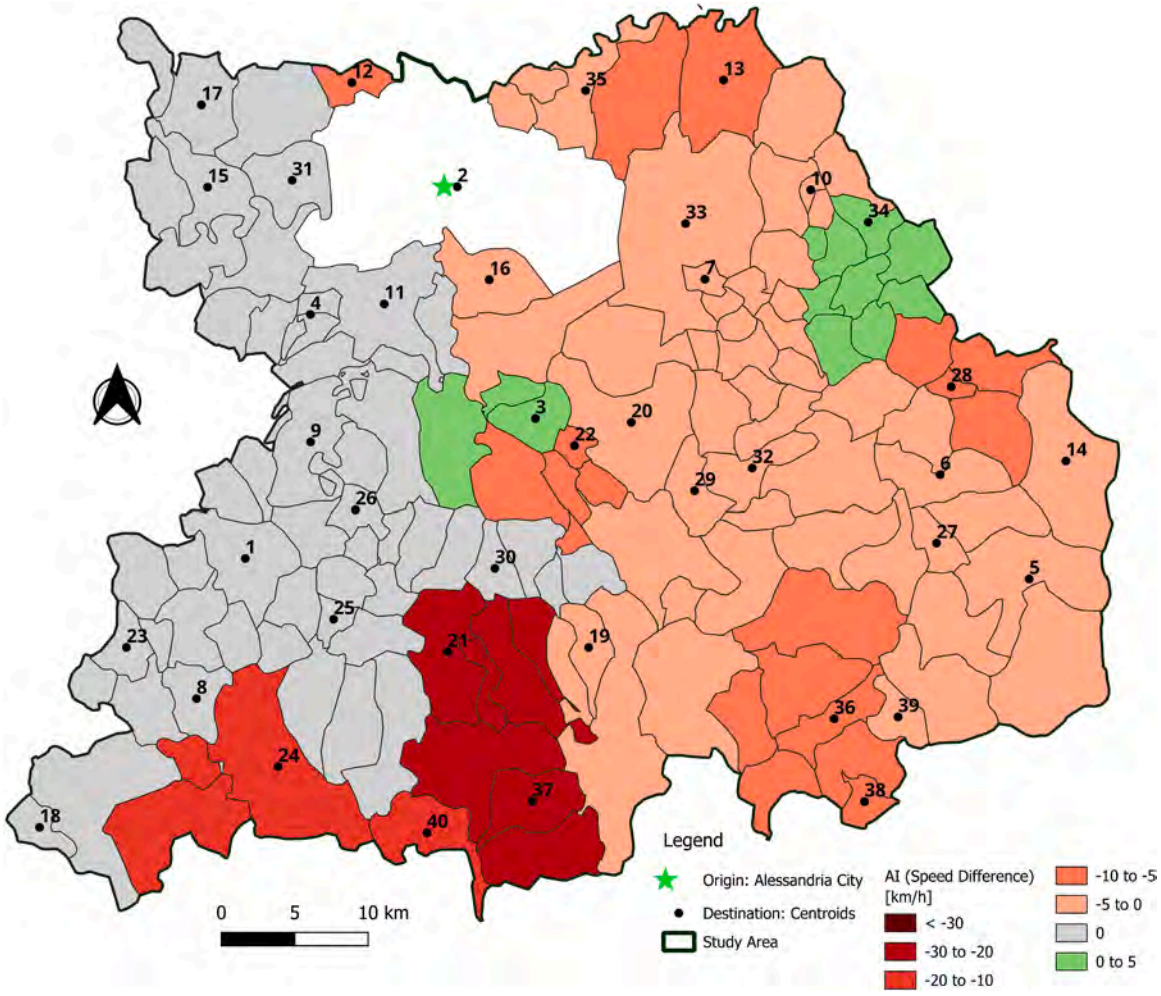


**Fig. 10.** Spatial and topological analysis: accessibility index difference of Alessandria city.

travel speeds of traffic flow for selected routes between entry and exit points along motorway sections that exhibit the highest traffic volumes. Only the motorway routes directly connecting these points are considered.

In the mesoscopic simulation using SUMO, it is possible to calculate the average speed of each route using outputs from edge-based result files. These outputs provide aggregated indicators such as mean vehicle speed, edge density, travel time, and edge length. This data forms the basis for computing average route speeds by dividing the total travel time across all edges of a route by the total route length.

To perform the validation, the average speed of traffic flow estimated by the mesoscopic simulation is compared with real-world data for the same routes and time period. One of the reliable sources of observed traffic data is the TomTom Move platform, which also provides traffic statistics including speed variations, travel time, demand, and congestion patterns across different road segments. Although this study primarily aims to utilise only free and publicly available datasets, the limited availability of up-to-date traffic data for the study area necessitated the use of this dataset solely for the purpose of model validation. Importantly, this dataset (Tom tom, Move) is not part of the core methodology developed for vulnerability assessment and does not compromise the open-data-based framework of the study. Both the proposed methods for vulnerability analysis remain fully applicable using only open-source software and publicly available datasets.

To quantify the accuracy of the mesoscopic simulation in predicting traffic speeds, the Mean Absolute Percentage Error (MAPE), a widely used metric for model validation (Shahdani et al., 2022), is calculated as follows:

$$MAPE\ (\%) = \frac{1}{n}\sum_{s=1}^{n}\left|\frac{S_t - S_m}{S_t}\right| * 100 \quad (4)$$

Where:

- n is the number of validated routes,
- $S_t$ is the average speed reported by TomTom for a given route,
- $S_m$ is the average speed predicted by the mesoscopic simulation.

## 4. Application of the methodology

### 4.1. Study area and data description

The study area is in the southern Piedmont region of northwest Italy, specifically within the province of Alessandria and some adjacent municipalities in the Liguria region. The total population of the study area is 342,964 covering an area of 3070.274 km$^2$. The municipality of Alessandria, with a population of 91,323, is the most important city in this region. Historical records document recurrent flood events, underscoring the area's vulnerability to hydrological hazards and the necessity for effective flood management strategies (Mandarino et al., 2021b).

Alessandria's road network plays a key role in regional transportation and connectivity. Key routes include the A21 motorway, which links Alessandria to Turin and Piacenza; the A7 motorway, connecting Milan to Genoa while crossing the province; the A26 motorway, which extends from Voltri to Gravellona, and several national roads

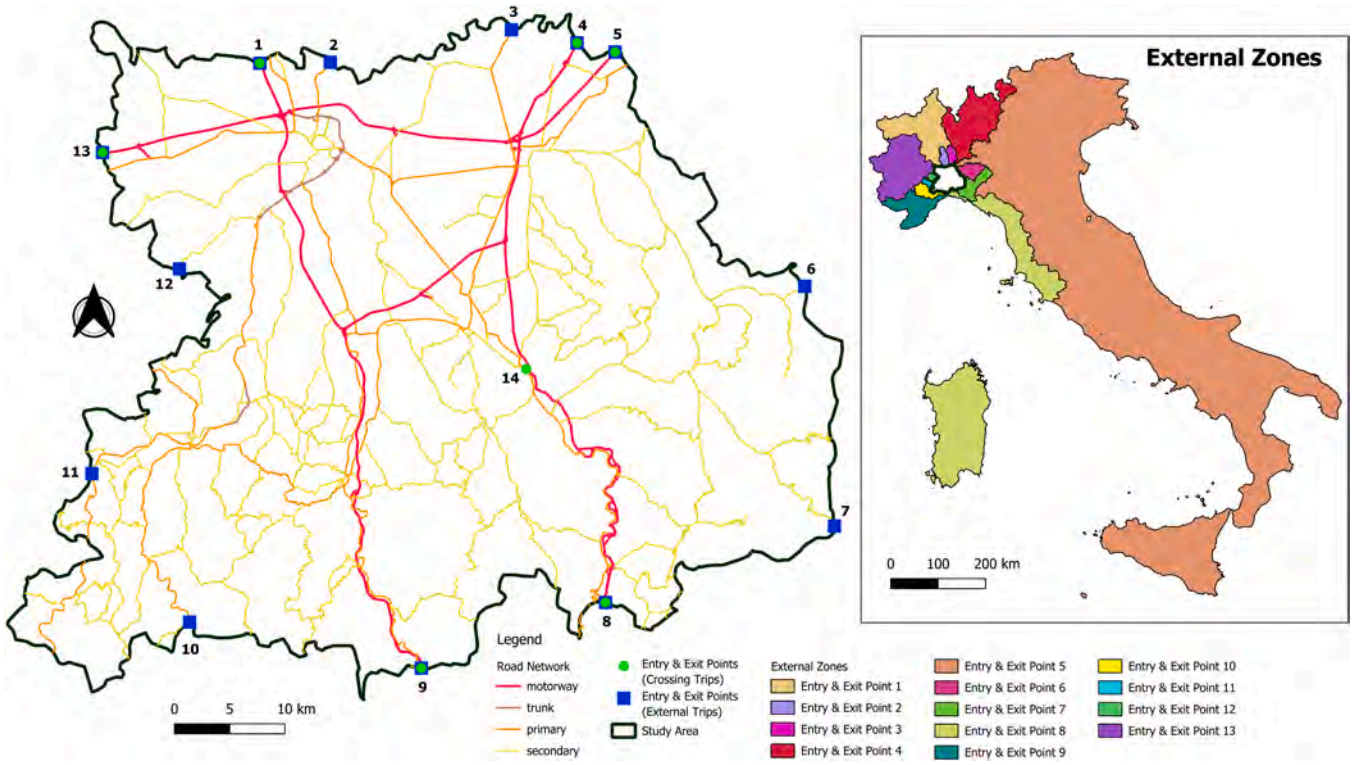


**Fig. 11.** Location of entry and exit points of the study area.

**Table 2**
Relevant entry and exit points of the study area.

| ID | Name | Road Class | Latitude | Longitude |
|---|---|---|---|---|
| 1 | A26_Autostrada dei Trafori | motorway | 44.9778437 | 8.54564034 |
| 2 | SS494_Strada Alessandria | primary | 44.9789083 | 8.62686787 |
| 3 | SS211_Strada statale della Lomellina | primary | 45.0058918 | 8.83484837 |
| 4 | A7_Autostrada dei Giovi-Serravalle | motorway | 44.9953213 | 8.91024785 |
| 5 | A21_Autostrada dei Vini | motorway | 44.9877889 | 8.95392025 |
| 6 | SP111 | secondary | 44.7969352 | 9.17150843 |
| 7 | SP147 | secondary | 44.6016105 | 9.20474144 |
| 8 | A7_Autostrada dei Giovi-Serravalle | motorway | 44.5395146 | 8.94337585 |
| 9 | A26_Autostrada dei Trafori | motorway | 44.4858357 | 8.73351167 |
| 10 | SP334_Strada provinciale del SASSELLO | primary | 44.5224518 | 8.46925598 |
| 11 | SP30 | primary | 44.64271 | 8.3564144 |
| 12 | SP240 | secondary | 44.8099838 | 8.45497758 |
| 13 | A21_Autostrada dei Vini | motorway | 44.9043332 | 8.365863 |
| 14 | A7_Autostrada dei Giovi-Serravalle | motorway | 44.7295531 | 8.85211617 |

**Table 3**
Crossing trips.

| From_Name | To_Name | From_ID | To_ID | Mesoscopic Simulation: Number (Veh/h) |
|---|---|---|---|---|
| Genova | Milano | 8 | 4 | 1330 |
| Gravellona | Voltri | 1 | 9 | 750 |
| Milano | Genova | 4 | 8 | 1330 |
| Milano | Serravalle | 4 | 14 | 830 |
| Milano | Voltri | 4 | 9 | 545 |
| Piacenza | Torino | 5 | 13 | 1111 |
| Serravalle | Milano | 14 | 4 | 830 |
| Torino | Piacenza | 13 | 5 | 1111 |
| Voltri | Gravellona | 9 | 1 | 750 |
| Voltri | Milano | 9 | 4 | 545 |

crossing the province. Fig. 3 illustrates the study area, including municipalities and their populations, along with the motorways.

Several rivers in the study area are prone to flooding, including the Tanaro, Bormida, Orba, and Torrente Scrivia rivers. As a result, the study area falls within multiple catchment areas: the Tanaro river in the northwest, the Belbo, Bormida, and Orba rivers in the south and southwest, the Scrivia and Curone rivers in the east and southeast, and the Po river in the north, as shown in Fig. 4. To assess the impact of flood events on road connectivity, particularly on motorways leading toward the Liguria region, some municipalities from Liguria within the Orba river catchment area were included in the study. This is particularly relevant for the A26 motorway, which connects Gravellona to Voltri and Genoa. In total, the study area comprises 146 municipalities, 134 in the Alessandria province and 12 in the Liguria region.

All shapefiles representing the study area, municipalities (Geoportal of Piedmont, Administrative areas), and catchment areas (Geoportal of Piedmont, Arpa Piemonte, Hydrographic basins) were obtained from the Geoportal of Piedmont as free and publicly available data. Additionally, river data was extracted from OpenStreetMap using the QuickOSM plugin in QGIS. QGIS software was used for spatial visualization and data processing, with all maps utilizing the WGS84 UTM Zone 32 N geographic coordinate system and the Universal Transverse Mercator (UTM) projection.

As the study area comprises 146 municipalities, considering each as a separate TAZ would result in an O-D skim matrix containing 21,316 elements. To enhance efficiency and improve analytical capabilities, a clustering approach introduced in Section 3.1 was adopted to reduce the number of zones while maintaining their connectivity within the road network. Municipalities were initially clustered using the k-means tool in QGIS, with distance as the clustering criterion, resulting in 40 clusters. Within each cluster, the municipality with the highest population density was selected as the representative TAZ, and its geometric centroid was designated as the representative centroid for that cluster.

**Table 4**
Basic statistics of mesoscopic simulation in baseline and disrupted scenarios.

| Parameters/Scenarios | Baseline Scenario | Disrupted Scenario |
|---|---|---|
| **Simulation Duration (s)** | 9582 | 10,205 |
| **Number of Loaded Vehicles (Total)** | 20,661 | 20,661 |
| **Number of Inserted Vehicles (Total)** | 20,661 | 20,635 |
| **Number of Vehicles (Running)** | 0 | 0 |
| **Number of Vehicles (Waiting)** | 0 | 0 |
| **Average Route Length (m)** | 38,205.91 | 48,626.97 |
| **% Difference** *((Disrupted scenario - Basic Scenario) / Basic Scenario)* | - | 27 % |
| **Average Duration (s)** | 1637.72 | 2806.53 |
| **% Difference** *((Disrupted scenario - Basic Scenario) / Basic Scenario)* | - | 71 % |
| **Total Travel Time (s)** | 33,836,951 | 57,912,646 |
| **% Difference** *((Disrupted scenario - Basic Scenario) / Basic Scenario)* | - | 71 % |
| **Average Speed (m/s)** | 23.27 | 19.27 |
| **% Difference** *((Disrupted scenario -Basic Scenario) / Basic Scenario)* | - | −17 % |
| **Teleported Vehicles (Wrong Lane)** | 0 | 0 |
| **Teleported Vehicles (Yield)** | 0 | 0 |
| **Teleported Vehicles (Jam)** | 47 | 183 |
| **Teleported Vehicles (Total)** | 47 | 183 |
| **% Reliability** | - | 99 % |
| **Average Waiting Time (s)** | 5.81 | 26.11 |
| **% Difference** *((Disrupted scenario - Basic Scenario) / Basic Scenario)* | - | 349 % |

Fig. 5 illustrates the clustered internal TAZs and their representative centroids, while Table 1 lists the names and IDs of these centroids. The aggregated centroids were also used for the post-processing of mesoscopic traffic simulation results, while trip generation was based on the detailed zoning version (without k-means clustering), as described in Section 4.3.

The road network used in both methodologies was obtained from freely available online data sources, OpenStreetMap (OSM), as shown in Fig. 6. While OSM offers an accessible and frequently updated source of road network information, its coverage and accuracy can vary across regions. In particular, rural and less-populated areas may have limited or outdated data due to lower contributor density. In this case study, the road network was initially inspected visually and cross-verified in the study area to ensure completeness and consistency. Both datasets include 13 road types classified as follows:

- Motorways: motorway, motorway_link
- Trunk roads: trunk, trunk_link
- Primary roads: primary, primary_link
- Secondary roads: secondary, secondary_link
- Local roads: tertiary, tertiary_link, unclassified, residential, living_street

In the spatial analysis approach, the road network consists of a total length of 6536.441 km, with 19,369 links and 25,547 nodes. In the simulation-based method, the road network extends to a total length of 11,510.033 km, with 46,619 links and 20,850 nodes considering multiple-lane roads. This difference is due to how the road network is represented in each environment: in QGIS, roads are typically modeled as bidirectional single-line features, while in SUMO, each direction is represented as a separate one-way edge. As a result, bidirectional roads become two separate links in SUMO, and multi-lane roads are further split, increasing the total number of links and overall network length. Additionally, these datasets contain attributes such as road length, presence of bridges and tunnels, road names, speed limits, one-way restrictions, traffic direction, and access permissions.

To extract trip information, two Italian datasets, ISTAT 2011 Census Data (Istituto Nazionale di Statistica, Commuting Matrices) and AISCAT 2023 Motorway Statistics (Associazione Italiana Società Concessionarie Autostrade e Trafori, Traffic flow on motorways) were utilized to define the traffic demand in the study area.

The ISTAT 2011 dataset provides an origin-destination matrix for

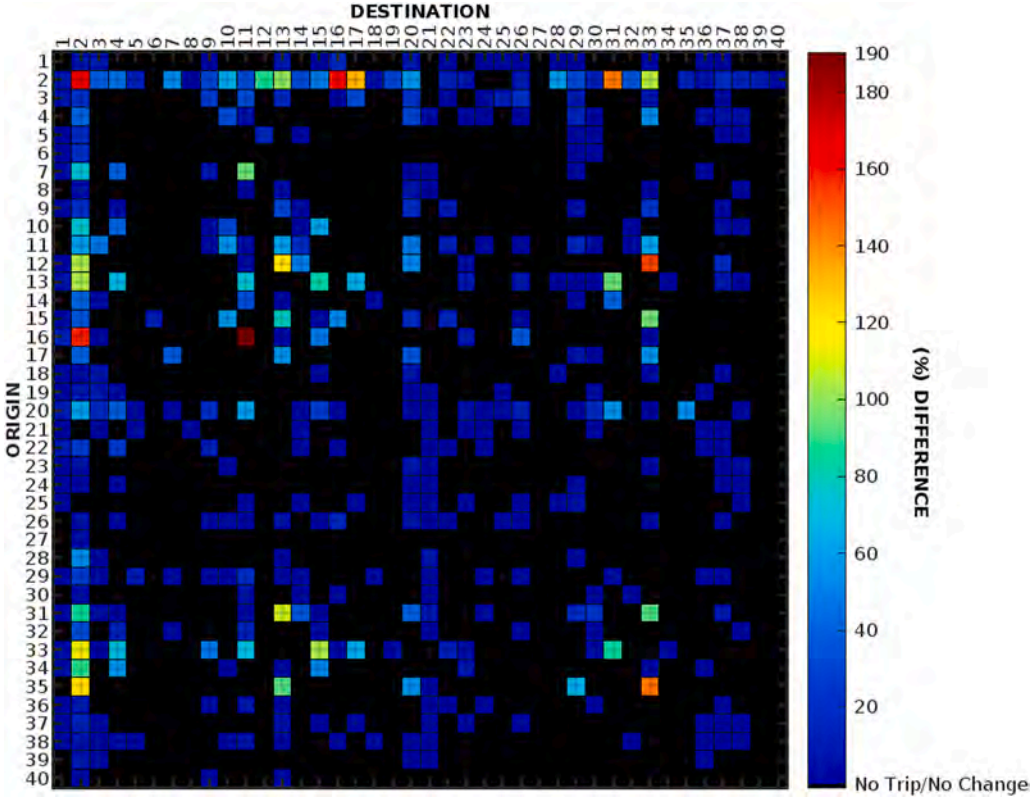


**Fig. 12.** Mesoscopic simulation analysis: O-D percentage cost difference skim matrix, distance impedance.

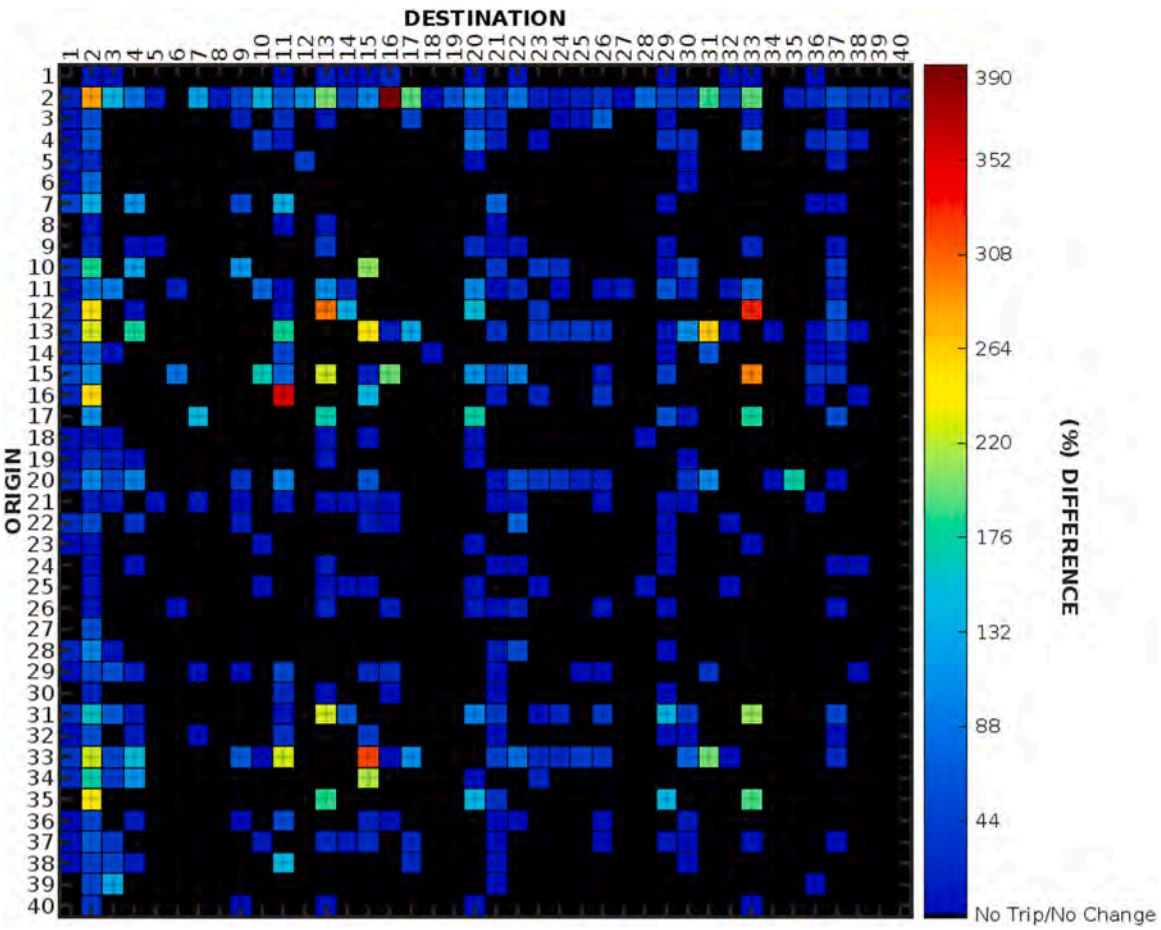


**Fig. 13.** Mesoscopic simulation analysis: O-D percentage cost difference skim matrix, time impedance.

daily movements related to work or study. It is based on data from the 15th General Population Census (reference date: October 9, 2011). The dataset covers 28,871,447 individuals who reported commuting daily to their usual place of study or work, returning to their residence. The dataset includes information on:

- The number of individuals traveling between or within municipalities.
- The purpose of the trip (work or study).
- Traveller gender.
- Mode of transport used.
- Departure time slots.
- Duration of the journey.

The AISCAT 2023 dataset provides traffic flow and accident data on Italian motorways. It includes statistics crucial for understanding the volume of traffic crossing the study area. Key metrics used in the dataset include:

- Actual vehicles: The total number of vehicle units (light and heavy vehicles) entering the motorway, regardless of the distance traveled.
- Vehicle-kilometers: The total kilometers traveled by all vehicles on the motorway.
- Theoretical vehicles: The estimated number of vehicles that, if traveling the entire motorway, would generate the same total vehicle-kilometers recorded. This is calculated as the ratio between total vehicle-kilometers and motorway length.

Therefore, by combining these two datasets, this study incorporates both census-based mobility patterns and motorway traffic flow data to define the traffic demand model for the study area.

To define a flood disrupted scenario for the study area, a floodplain map (Fig. 4) was utilized, focusing on the province of Alessandria to assess the road network's vulnerability to flooding. A vector shapefile layer was obtained from ARPA Piemonte (The Regional Agency for Environmental Protection of Piedmont) and downloaded from the Geoportal of Piedmont website (Geoportal of Piedmont, Arpa Piemonte, Floodable areas). This dataset provides information on potentially floodable areas in the Piedmont region, categorized based on flood return periods and the type of material deposited in flood-prone zones. The dataset originates from the analysis of historical archive documents related to past flooding events and systematic interpretative studies of aerial photographs conducted in the Piedmont region until the 1990s. By incorporating this flood data, the study evaluates the impact of flooding events on road network functionality and identifies critical vulnerabilities.

### 4.2. Results of spatial and topological analysis

Following the steps shown in Section 3.5, the baseline road network model was completed. The next step was to assess its performance by creating disrupted scenarios to evaluate vulnerabilities. By analysing the floodplain map shown in Fig. 4, it was evident that the Tanaro, Orba, and parts of the Bormida rivers are the most flood-prone areas, flooding approximately every 3 to 5 years. By overlaying the flood map with a vector shapefile containing links over bridges extracted from the road network dataset using the bridge field, it was identified that twelve bridges, distributed across the catchment areas of the Tanaro River (7 bridges), Bormida River (2 bridges), and Orba River (3 bridges), are in flood-prone areas within this return period. To simulate a real-world

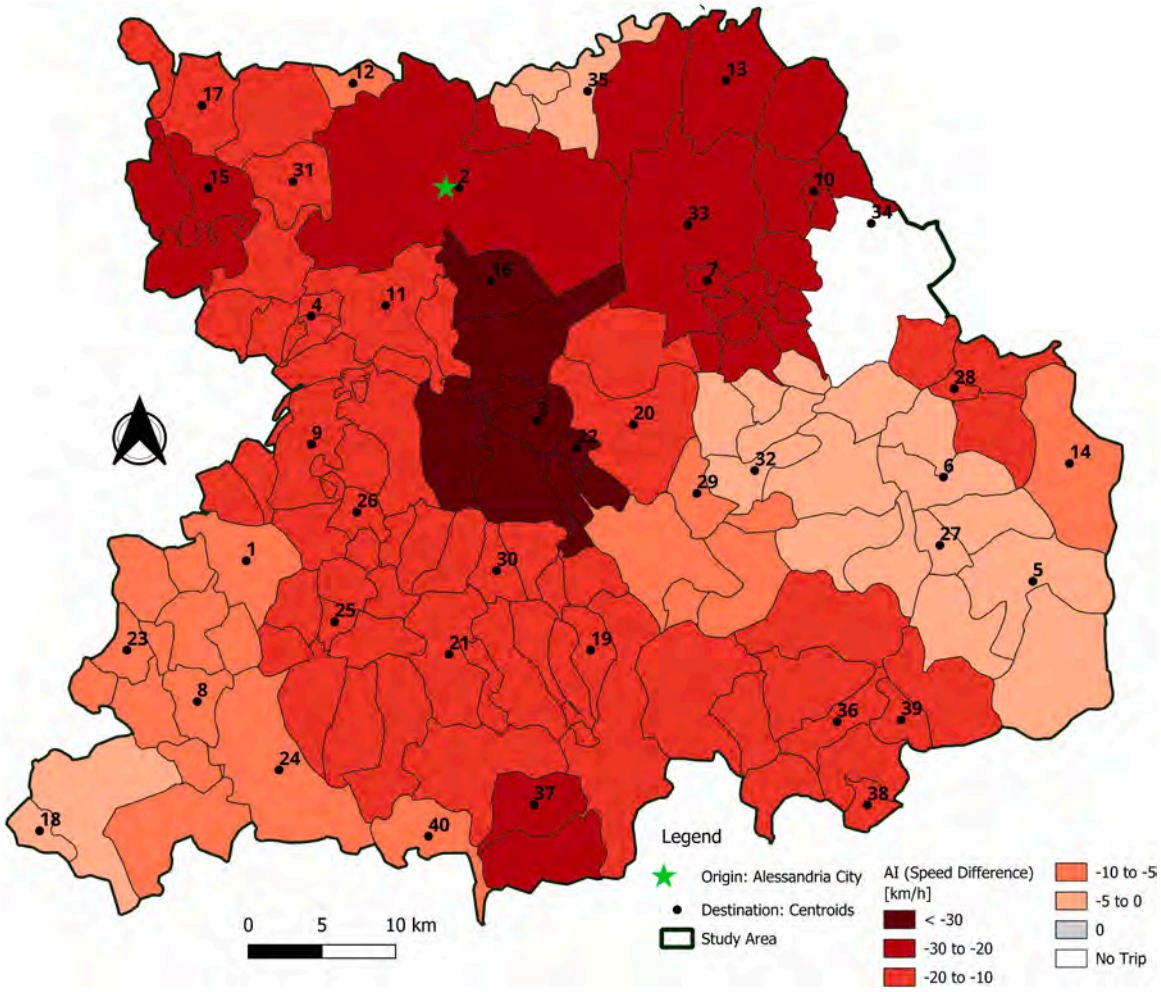


**Fig. 14.** Mesoscopic simulation analysis: accessibility index difference of Alessandria city.

disruption, 52 edges over the bridges were closed in the spatial and topological model, and closures were propagated along affected road segments (covering 264 graph edges) until the first entry or exit point of the road network. This approach was particularly necessary for motorways, where closures were extended up to the first interchange, reflecting real-world conditions where drivers need to be alerted about closures in advance to change their routes. Fig. 7 illustrates the disrupted scenario, the disrupted road network, and closed bridges within the study area.

To quantify the road network vulnerability using serviceability-based methods, the O-D skim cost matrix for both the baseline and disrupted scenarios was calculated, considering both distance and time impedances. The percentage cost difference was then calculated, as illustrated in Fig. 8 for distance impedance and Fig. 9 for time impedance.

As evident from the O-D percentage cost difference skim matrices, there is a general increase in both travel distance and travel time between most pairs of representative centroids. However, the increase is more pronounced in terms of travel time. In certain cases, there is no significant increase in travel distance, but the impact on travel time is more tangible due to rerouting through lower-speed roads in the disrupted scenario.

Trips originating from most representative centroids and heading toward Alessandria city (ID 2), the main municipality in the study area, experience a rise in both distance and travel time. This is primarily due to the closures along motorways A21 and A26, especially at their intersections with the Tanaro River. For instance, the travel time between centroid ID 16 (located in the central part of the study area) and Alessandria city (ID 2) has increased by over 200 %, while the travel distance has increased by >350 %. Additionally, trips originating from centroids ID 10, 13, 33, and 35 are notably affected in terms of both travel time and distance when traveling toward Alessandria city and among each other.

To evaluate road network vulnerability using accessibility-based methods, the Shortest Path tool from the Network Analysis toolbox in QGIS was employed to generate the fastest path tree (time impedance) from Alessandria municipality (ID 2) to other representative centroids in the study area for both the baseline and disrupted scenarios. For each scenario, the Accessibility Index was calculated based on the distance and travel time of the generated routes.

By comparing the AI across the two scenarios, as shown in Fig. 10, significant reductions in speed are observed for trips originating from Alessandria city (ID 2) towards other centroids. There is a notable speed reduction of 20–30 km/h for trips heading to southern zones, especially those that rely on the A26 motorway, which may be closed during flood events affecting the Tanaro, Orba, and Bormida Rivers. Additionally, accessibility has also decreased for northeastern zones due to the closure of the A21 motorway at its intersection with the Tanaro River in the disrupted scenario.

Contrary to initial expectations, some municipalities in the central and eastern parts of the study area experience a slight improvement in their AI, with speeds increasing by <5 km/h. Further analysis reveals that this unexpected improvement is attributed to route selection. In the disrupted scenario, both travel time and distance increased in

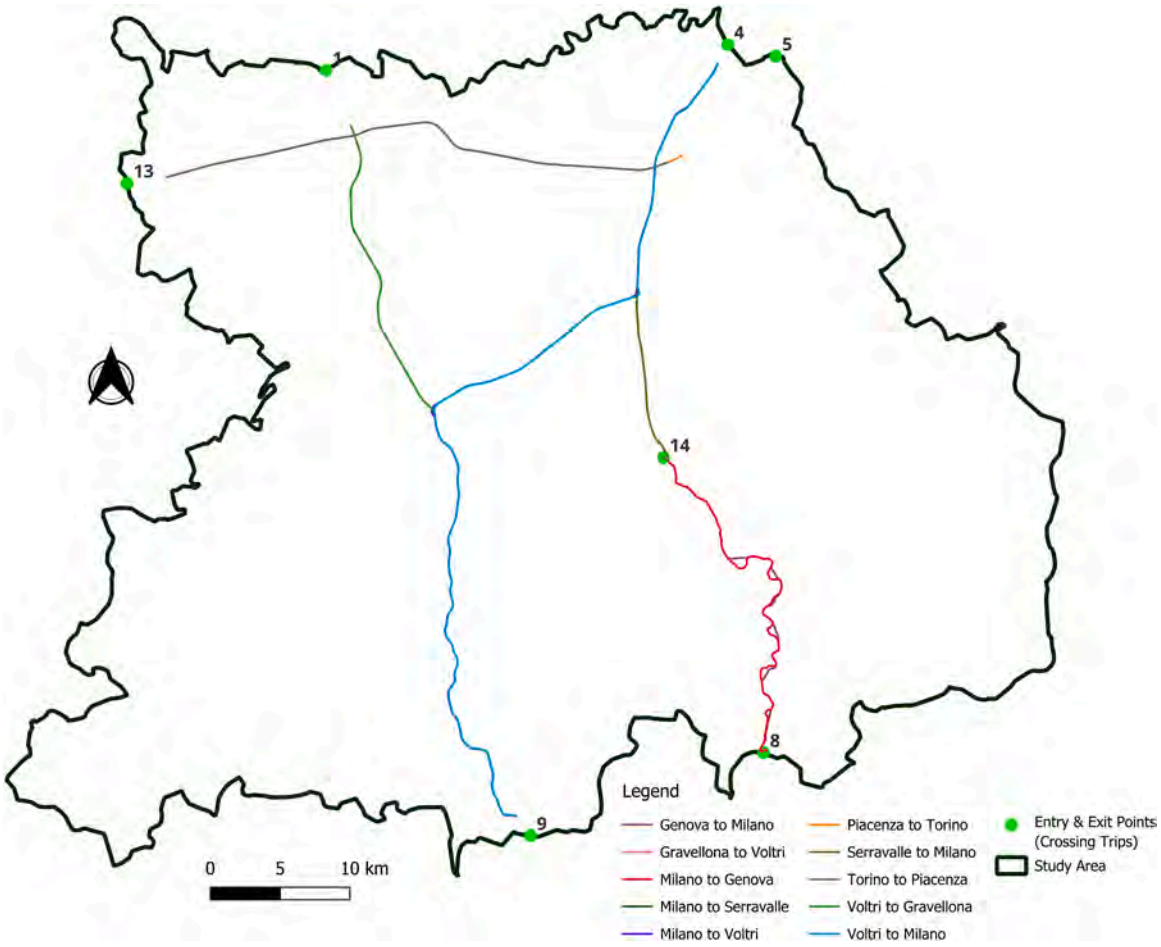


**Fig. 15.** Crossing trip routes.

comparison with the baseline scenario; however, the ratio of distance to time shows a slight growth. In the baseline scenario, the route primarily utilizes primary and mostly secondary roads. However, in the disrupted scenario, road closures redirect the route toward motorways, trunk roads, and primary roads. Given the higher speed limits of motorways compared to other road classes, this indirect improvement in the AI for certain municipalities is considered reasonable.

Another consideration in this spatial and topological approach is that trips originate and end at centroids. As a result, the vulnerability of intra-zonal trips (trips that start and end within the same zone) cannot be quantified using this methodology. To evaluate intra-zonal trips vulnerability, a finer TAZ division would be required, which would increase computational effort and costs.

### *4.3. Results of mesoscopic traffic simulation*

Starting from the defined study area and internal TAZs, traffic demand data were disaggregated into internal, external, and crossing trips. To accurately model and simulate external and crossing trips, it was necessary to define external zones and identify key entry and exit points to the study area. The main road edges that cross the study area, including motorways A21, A26, and A7, along with several national roads, were identified as entry and exit points. In total, 13 boundary points were defined at the study area's perimeter (Fig. 11), with an additional entry and exit point inside the study area to model crossing trips exclusively for motorway A7. These points serve as locations where:

- External trips originate (from external zones to internal TAZs) or terminate (from internal TAZs to external zones).
- Crossing trips begin and end at these defined points (edges), meaning that vehicles do not stop within the study area but rather pass through it.

To determine the external zones, spatial data processing was performed in QGIS using a shapefile layer containing municipality boundaries for the entire country of Italy (Istituto Nazionale di Statistica, Administrative areas). By overlapping this layer with the shapefile of the entry and exit points, all municipalities outside the study area were designated as 13 external zones, which are linked to the study area through the entry and exit points. Table 2 presents the entry and exit points, while Fig. 11 illustrates these points along with the external zones.

To model the traffic demand in the study area, two Italian datasets were utilized: ISTAT 2011 and AISCAT 2023. By querying the complete commuting matrix from ISTAT 2011, all trips originating and terminating within the 146 municipalities inside the study area were identified. This study focused on private vehicles, including cars and motorcycles. The trip purposes, as outlined in Section 4.1, were categorized into home-based work (HBW) and home-based education (HBE). Additionally, the exit time parameter was considered to simulate morning rush hour conditions, specifically between 07:15 and 08:15 in the morning, as this timeframe corresponds to the peak commuter period, ensuring the highest vehicle injection rates into the road network.

This process resulted in two tables displaying the probability of each TAZ serving as either an origin or a destination of internal trips. These

**Table 5**
Results of the validation procedure.

| From_Name | To_Name | From_ID | To_ID | Simulation: Travel Length (km) | Simulation: Travel Time (h) | Simulation: Average Speed (km/h) | Observation: Travel Length (km) | Observation: Travel Time (h) | Observation: Average Speed (km/h) | Difference: Average Speed (km/h) | % Difference: Average Speed ( %) |
|---|---|---|---|---|---|---|---|---|---|---|---|
| Genova | Milano | 8 | 4 | 58.22 | 0.68 | 85.47 | 58.36 | 0.54 | 108.52 | 23.05 | 21.24 |
| Gravellona | Voltri | 1 | 9 | 54.88 | 0.57 | 95.50 | 55.02 | 0.55 | 100.30 | 4.80 | 4.78 |
| Milano | Genova | 4 | 8 | 61.14 | 0.81 | 75.93 | 61.51 | 0.62 | 99.13 | 23.21 | 23.41 |
| Milano | Serravalle | 4 | 14 | 30.69 | 0.35 | 87.07 | 30.88 | 0.27 | 114.84 | 27.77 | 24.18 |
| Milano | Voltri | 4 | 9 | 67.68 | 0.72 | 93.56 | 67.95 | 0.67 | 101.43 | 7.87 | 7.76 |
| Piacenza | Torino | 5 | 13 | 37.78 | 0.37 | 102.89 | 38.07 | 0.34 | 111.06 | 8.17 | 7.36 |
| Serravalle | Milano | 14 | 4 | 30.85 | 0.33 | 93.06 | 30.94 | 0.26 | 117.51 | 24.45 | 20.80 |
| Torino | Piacenza | 13 | 5 | 37.17 | 0.37 | 99.76 | 37.20 | 0.34 | 107.99 | 8.22 | 7.61 |
| Voltri | Gravellona | 9 | 1 | 54.64 | 0.56 | 97.69 | 54.87 | 0.48 | 115.35 | 17.66 | 15.31 |
| Voltri | Milano | 9 | 4 | 67.59 | 0.71 | 95.17 | 67.83 | 0.59 | 115.03 | 19.85 | 17.26 |

values were then incorporated into QGIS, and probabilities were assigned to each edge, determining their likelihood of being an origin or destination of internal trips. These probability tables were subsequently employed to control the distribution of origins and destinations for the generated random internal trips in the mesoscopic simulation.

In addition to internal trips, two layers of traffic demand were created to define external trips based on the random trip method and ISTAT 2011 data. The first layer represented trips originating within the study area (internal TAZs) and traveling to municipalities outside the study area (external zones). Conversely, the second layer encompassed trips originating in external zones and terminating within internal TAZs. Each external zone was linked to a predefined entry and exit point (Fig. 11). By integrating external zone information with the external trip dataset, each trip was assigned a corresponding entry or exit point.

Crossing trips were also considered along the three major motorways (A21, A26, and A7) using average daily traffic flow data from the AISCAT 2023 dataset, specifically considering theoretical vehicle counts for light vehicles. These trips were simulated by defining traffic flows between entry and exit points over motorways. To represent peak-hour conditions, it was assumed that approximately 10 % of the Annual Average Daily Traffic (AADT) occurred during the morning rush hour, with traffic distributed uniformly in both directions on the motorways. Table 3 shows the number of vehicles per hour assigned as traffic flow to the motorways, including the crossing trips to the study area.

Overall, the study accounted for 7245 internal trips, 2200 external trips originating within the study area and heading outside, and 2200 external trips entering from external zones, all during the 07:15 to 08:15 morning rush hour. To align with this peak period, random trip generation in the simulation was set to occur over a 3600-second (one-hour) interval. After merging the internal and external trips, an additional 9132 crossing trips along the motorways were integrated into the demand dataset as direct flows between their respective origin and destination edges (entry and exit points), creating the complete trip dataset required for the mesoscopic simulation.

The finalized traffic demand was applied to both the baseline and disrupted scenarios, and mesoscopic simulations were conducted in SUMO. A constant demand assumption was maintained, meaning that users did not alter their travel mode in response to flooding conditions. While it is true that this is a strong assumption, the lack of available data on modal shifts due to flood-related closures justified its use. Therefore, it was assumed that all users maintained their original mobility decisions. This approach allows the analysis to represent an extreme, yet safety-oriented scenario: what would be the network impacts if all travellers still chose to move using their intended mode of transport, despite disruptions? Additionally, in the disrupted scenario, the rerouter function was implemented to ensure that all 52 identified edges over the 12 bridges affected by flooding scenario remained closed throughout the simulation. This approach effectively modelled the impact of road closures on travel patterns and network performance.

The aggregated data of the mesoscopic simulations, summarized in Table 4, reveal that the overall simulation time increased in the disrupted scenario, indicating a longer duration required for vehicles to leave the road network. Additionally, a slight reduction in the number of inserted vehicles was observed, as some trips could not begin since their origins were located on closed links. Notably, both average travel distance and travel time increased in the disrupted scenario compared to the baseline, while the average speed decreased. These findings emphasize the vulnerability of the road network in Alessandria when subjected to flooding events. Moreover, the number of teleported vehicles increased in the disrupted scenario, primarily due to congestion and traffic jams. While an increase in teleportation is generally a negative indicator, the overall network reliability remained high, with 99 % of inserted vehicles successfully reaching their destinations without being teleported. However, a significant rise in average waiting time, approximately 350 %, was observed in the disrupted scenario, further highlighting the impact of flooding on road network performance and its

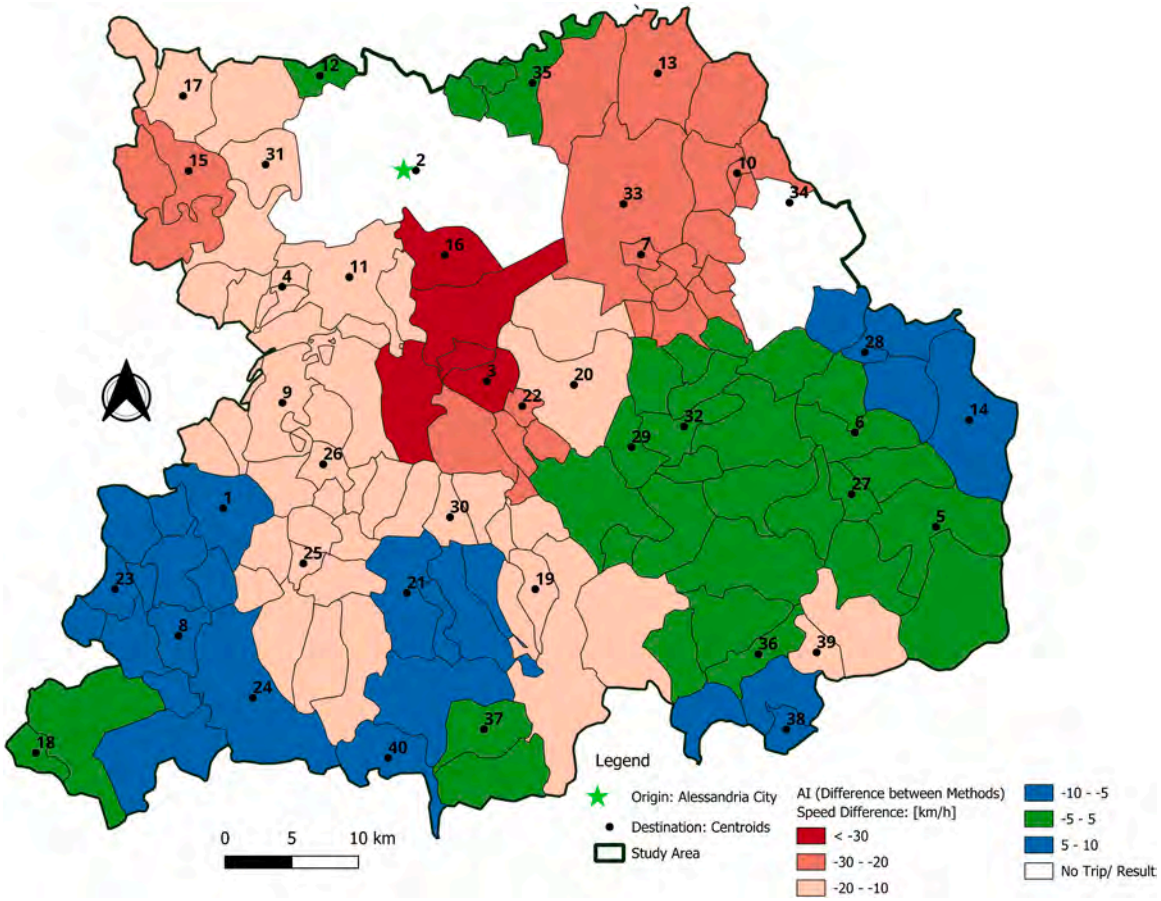


**Fig. 16.** Difference in Accessibility Index between mesoscopic simulation analysis and spatial and topological analysis methods for Alessandria city.

capacity to accommodate peak-hour traffic under flooding conditions.

The trip data was aggregated into 40 representative centroids, forming an O-D skim cost matrix that captured both distance and time impedance under baseline and disrupted scenarios. The percentage cost difference between the two scenarios was then computed, as illustrated in Fig. 12 for distance impedance and Fig. 13 for time impedance.

The resultant matrices indicate a general increase in both travel distance and travel time between most pairs of representative centroids in the disrupted scenario. However, the increase in travel time is notably more pronounced. Trips from various representative centroids to Alessandria city (ID 2) exhibit significant cost increases in both metrics. For instance, the travel time between Alessandria municipality (ID 2) and centroid ID 16 increased by over 350 %, while the corresponding travel distance increased by >170 %.

Furthermore, the simulation approach models the trips as originating and terminating at centroids, allowing for an assessment of intra-zonal travel disruptions. The vulnerability of intra-zonal trips is particularly evident in the results. As shown in Fig. 12 and Fig. 13, intra-zonal trips within Alessandria city (ID 2) experienced a travel distance increase of over 150 % and a travel time increase of nearly 300 %, underscoring the impact of disruptions on localized mobility.

By analyzing the average trip duration and distance for all trips originating from Alessandria city towards the representative centroids, the AI difference between the baseline and disrupted scenarios was computed. This difference, expressed as a reduction in average speed (km/h), is illustrated in Fig. 14.

#### *4.3.1. Validation of the mesoscopic model*

To validate the mesoscopic simulation model under baseline (non-flooded) conditions, 10 routes were identified among 7 entry and exit points connected to the motorway network. These routes are the same as those used for assigning traffic flow on the motorways, as described in Table 3 and illustrated in Fig. 15.

The average travel speed predicted by the simulation for each route was calculated using edge-based output data from the mesoscopic simulation model. Specifically, the sum of aggregated travel times of all edges along a given route was obtained, and the total route length was divided by this value to estimate the mean travel speed. For the same set of routes, real-world travel speed data was collected from the TomTom Move platform. The data corresponds to August 2024 for the same geographic region, and the time window of 07:00 to 08:00 a.m. was selected, aligning with the simulated demand period in the study.

Using this information, the MAPE was calculated for the 10 selected routes using Eq. (4). Table 5 shows the travel time, route length, and average speed based on both the mesoscopic simulation results and the TomTom data. The resulting MAPE value was 14.9 %, which indicates a reasonably good level of agreement between the simulated and observed traffic conditions.

Overall, this result supports the reliability of the simulation model, despite potential sources of uncertainty. These uncertainties stem from the use of only free and publicly available datasets and from extending the model to a large regional area encompassing 146 municipalities. Nonetheless, the relatively low validation error suggests that the model provides a solid basis for integration with flood scenarios.

### 4.4. Discussion

A comparison of the O-D percentage cost difference skim matrix (distance and time impedance) derived from the mesoscopic simulation of traffic demand (Fig. 12 and Fig. 13) with the results of the spatial and

topological approach (Fig. 8 and Fig. 9) reveals a generally consistent pattern in travel cost increases between the baseline and disrupted scenarios. For example, in the spatial and topological analysis, the O-D pair between Alessandria city (ID 2) and centroid (ID 16) exhibited more than a twofold increase in travel time under the disrupted scenario. This trend is reflected in the mesoscopic traffic simulation results, where travel demand is explicitly considered. In this case, the average travel time between these O-D pairs more than tripled when traveling from centroid ID 2 to centroid ID 16 and more than doubled when traveling in the opposite direction. Additionally, trips originating from centroids ID 13, 33, and 35 showed considerable increases in travel time when heading towards Alessandria municipality.

Fig. 16 illustrates the difference in AI difference values between the two methods (AI difference from the mesoscopic simulation (Fig. 14) minus AI difference from the spatial and topological analysis (Fig. 10)). A threshold of 5 km/h was assumed to classify negligible differences in speed reduction, while 10 km/h was used to denote partially similar patterns of accessibility changes across the study area. The difference in speed reduction between the two methods for trips to the southern part of the study area remains within the range of −10 km/h to +10 km/h, while for some southeastern and northern zones the difference is even smaller (−5 to +5 km/h).

While the spatial and topological method shows no notable decrease in accessibility when traveling westward from Alessandria city, the mesoscopic simulation indicates a noticeable speed reduction of 10–20 km/h in this direction (Fig. 16). Furthermore, whereas the spatial and topological approach suggests a slight increase in speed for trips from Alessandria city to centroid ID 3 in the center of the study area, the mesoscopic simulation highlights a speed reduction exceeding 30 km/h, reflecting the network's sensitivity to disruptions when demand is considered.

Overall, Fig. 16 suggests that trips from Alessandria city (ID 2) to the southern part of the study area display a consistent pattern of reduced speed across both methods. By contrast, trips toward the west and northeast show differences of 10–20 km/h and 20–30 km/h, respectively, between the AI difference obtained with the two methodologies. In the central neighbouring municipalities, the mesoscopic simulation reveals substantially higher speed reductions, exceeding 30 km/h, underlining the role of traffic demand integration in the analysis.

Moreover, while the spatial and topological method is unable to capture accessibility changes for intra-zonal trips within Alessandria city, the mesoscopic simulation effectively reveals reduced accessibility within the municipality (Fig. 14), particularly due to bridge closures over the Tanaro and Bormida Rivers. This highlights the advantage of including traffic simulation in the analysis, as it provides a more detailed and dynamic assessment of network vulnerabilities under disrupted conditions. This limitation of the spatial and topological analysis could indeed be addressed by refining and detailing the TAZ division; however, doing so would significantly increase computational effort. The use of larger TAZs results in a loss of intra-zonal trips, which can be partially mitigated, but not fully resolved, by increasing the number of zones. Nonetheless, this comes at the expense of macroscopic feasibility for large-area assessments. Additionally, the selection and placement of representative centroids may introduce the Modifiable Areal Unit Problem (MAUP), as results can vary depending on the location of the centroids (Viegas et al., 2009). However, it is important to emphasize that the objective of this study and its case application was not to eliminate such spatial uncertainties, but rather to apply and compare the methodologies employed in evaluating network vulnerability. In particular, the results are obtainable with different levels of methodology complexity and data availability.

Overall, in the Alessandria case study, using both methodologies, the road network affected by the 3 to 5-year flood events occurring in the Tanaro, Orba, and Bormida rivers is generally reliable but can be heavily vulnerable. These flood events lead to increased travel time and distance between origin and destination pairs, especially for trips starting and ending in Alessandria city, which is notably affected by flooding events in the Tanaro River. Furthermore, the Orba River impacts the A26 motorway and its connection to the A7, resulting in decreased accessibility to the southern parts of the study area.

## 5. Conclusion

Road networks are fundamental to the functioning of society and the vulnerability of interconnected infrastructure systems, playing a crucial role in daily mobility, transportation of goods, and emergency response. Given the increasing frequency and unpredictability of extreme flood events, it is imperative to assess the vulnerability of road networks and develop adaptive strategies to reduce disruptions and their effects.

Several studies have assessed the effects of extreme flood events on road networks, highlighting their severe impacts on traffic disruption. This study compared two methodologies for evaluating road network vulnerability to flood-induced disruptions: a GIS-based spatial and topological analysis and a mesoscopic traffic simulation approach. These methodologies aim to be easily applicable by authorities and transport planners for quickly assessing road network vulnerability in the days following flood events, particularly at a regional scale. The spatial and topological method enabled a rapid evaluation of network weaknesses without relying on traffic demand data, providing an efficient tool for quantifying vulnerabilities

Conversely, the mesoscopic traffic simulation approach offered a more detailed analysis by incorporating traffic demand, enabling the evaluation of congestion effects, travel time variations, and alternative routes under disrupted conditions. The simulation results highlighted the impact of flooding on network performance, with a 71 % increase in total travel time, a 27 % increase in travel distance, and a 17 % decrease in average speed. The accessibility index analysis further confirmed reduced mobility, particularly in areas dependent on flood-affected bridges. Additionally, the simulation method captured the impacts on intra-zonal traffic demand, which the spatial and topological method could not account for. The comparison between these two approaches emphasized the value of integrating traffic demand data and simulation tools, where available, to enhance the accuracy of vulnerability assessments.

The analysis of the O-D percentage cost difference skim matrix from the mesoscopic simulation method revealed that some centroid pairs exhibited no traffic demand. This was primarily due to the adopted logic used to build the mobility dataset, which focused on home-based work and education trips. Expanding the traffic demand data to include a broader range of internal, external, and crossing trips, beyond just home-based trips, would provide a more comprehensive understanding of road network vulnerability, particularly when analysing different time intervals outside peak hours.

Future research should focus on several key areas to enhance road network vulnerability assessments. First, the integration of dynamic flood maps would allow for time-dependent analysis, particularly for rapidly evolving flood events such as flash floods. Second, a systematic evaluation of individual bridge closures could support retrofitting efforts by identifying the most critical connections in the network at a regional scale. In addition, assessing the vulnerability of public and multimodal transportation systems as well as private motor vehicles would provide a more comprehensive assessment of the impacts of an extreme event on the study area. These advancements would strengthen the ability of authorities and transport planners to develop effective mitigation strategies, ultimately reducing infrastructure vulnerability against extreme events.

## CRediT authorship contribution statement

**Amirehsan Charlang Bakhtyari:** Writing – review & editing, Writing – original draft, Visualization, Validation, Software, Methodology, Formal analysis, Data curation, Conceptualization. **Angela**

**Carboni:** Writing – review & editing, Writing – original draft, Validation, Supervision, Methodology, Conceptualization. **Francesco Deflorio:** Writing – review & editing, Writing – original draft, Visualization, Validation, Supervision, Project administration, Methodology, Conceptualization. **Matteo Ferraro:** Writing – review & editing, Validation, Software, Formal analysis, Data curation, Conceptualization. **Lorenzo Sica:** Writing – review & editing, Methodology, Conceptualization.

## Declaration of competing interest

The authors declare the following financial interests/personal relationships which may be considered as potential competing interests: Francesco Deflorio and Matteo Ferraro reports financial support was provided by Ministry of University and Research (PRIN 2022 program). Angela Carboni reports financial support was provided by Ministry of University and Research (FSE REACT-EU-PON Ricerca e Innovazione). If there are other authors, they declare that they have no known competing financial interests or personal relationships that could have appeared to influence the work reported in this paper.

## Acknowledgements

This study was partially carried out within the FLOOD@ROAD project funded by the Ministero dell'Università e della Ricerca –within the PRIN 2022 program (D.D.104 −02/02/2022). This manuscript reflects only the authors' views and opinions, and the Ministry cannot be considered responsible for them. The research activity of A. Carboni was carried out within the Ministerial Decree no 1062/2021 and received funding from FSE REACT-EU-PON "Ricerca e Innovazione" 2014–2020.

## Data availability

Data for GIS-based spatial vulnerability analysis in the area of Alessandria in Italy in case of road network disruption (Original data) (Mendeley Data)

Data for the traffic flow simulation in the area of Alessandria in Italy in case of road network disruption (Original data) (Mendeley Data)

## References

Aghababaei, M., Costello, S. B., & Ranjitkar, P. (2020). Transportation impact assessment following a potential Alpine fault earthquake in New Zealand. *Transportation Research Part D: Transport and Environment, 87*, Article 102511. https://doi.org/10.1016/j.trd.2020.102511

(Siavash) Aghababaei, M. T, Costello, S. B., & Ranjitkar, P. (2021). Measures to evaluate post-disaster trip resilience on road networks. *Journal of Transport Geography, 95*, Article 103154. https://doi.org/10.1016/j.jtrangeo.2021.103154.

Alam, Md. S., Kim, K., Horner, M. W., Alisan, O., Antwi, R., & Ozguven, E. E. (2024). Large-scale modeling of hurricane flooding and disrupted infrastructure impacts on accessibility to critical facilities. *Journal of Transport Geography, 116*, Article 103852. https://doi.org/10.1016/j.jtrangeo.2024.103852

Associazione Italiana Società Concessionarie Autostrade e Trafori, Traffic flow on motorways. (n.d.). Retrieved February 28, 2025, from https://www.aiscat.it/2023/12/29/aiscat-informazioni-edizione-semestrale-1-2-2023/.

Balijepalli, C., & Oppong, O. (2014). Measuring vulnerability of road network considering the extent of serviceability of critical road links in urban areas. *Journal of Transport Geography, 39*, 145–155. https://doi.org/10.1016/j.jtrangeo.2014.06.025

Berdica, K. (2002). An introduction to road vulnerability: What has been done, is done and should be done. *Transport Policy, 9*(2), 117–127. https://doi.org/10.1016/S0967-070X(02)00011-2

Bi, W., Hackl, J., & MacAskill, K. (2025). Enhancing flood resilience of urban rail transit systems through recovery resource scheduling optimisation: A case study of London. *Sustainable Cities and Society, 128*, Article 106437. https://doi.org/10.1016/j.scs.2025.106437

Borowska-Stefańska, M., Bartnik, A., Dulebenets, M. A., Kowalski, M., Sahebgharani, A., Tomalski, P., & Wiśniewski, S. (2024). Changes in intra-city transport accessibility accompanying the occurrence of an urban flood. *Transportation Research Part D: Transport and Environment, 126*, Article 104040. https://doi.org/10.1016/j.trd.2023.104040

Brath, A., Casigli, N., Marani, M., Mercogliano, P., & Motta, R. (2023). *Rapporto della Commissione Tecnico-Scientifica Istituita con Deliberazione della Giunta Regionale n.984/2023. Al Fine di Analizzare gli Eventi Meteorologici Estremi del Mese di Maggio 2023; Regione EmiliaRomagna: Bologna, Italy, 2023; p. 147*.

Buzzi, A., Tartaglione, N., & Malguzzi, P. (1998). Numerical simulations of the 1994 Piedmont flood: Role of orography and moist processes. *Monthly Weather Review, 126*(9), 2369–2383. https://doi.org/10.1175/1520-0493(1998)126<2369:NSOTPF>2.0.CO;2

Ceccato, R., Deflorio, F., Diana, M., & Pirra, M. (2020). Measure of urban accessibility provided by transport services in Turin: A traveller perspective through a mobility survey. *Transportation Research Procedia, 45*, 301–308. https://doi.org/10.1016/j.trpro.2020.03.020

Cremonini, L., Randi, P., Fazzini, M., Nardino, M., Rossi, F., & Georgiadis, T. (2024). Causes and impacts of flood events in Emilia-Romagna (Italy) in May 2023. *Land, 13*(11), 1800. https://doi.org/10.3390/land13111800

Curl, A., Nelson, J. D., & Anable, J. (2015). Same question, different answer: A comparison of GIS-based journey time accessibility with self-reported measures from the National Travel Survey in England. *Computers, Environment and Urban Systems, 49*, 86–97. https://doi.org/10.1016/j.compenvurbsys.2013.10.006

Ding, W., & Wu, J. (2023). Interregional economic impacts of an extreme storm flood scenario considering transportation interruption: A case study of Shanghai, China. *Sustainable Cities and Society, 88*, Article 104296. https://doi.org/10.1016/j.scs.2022.104296

Evans, B., Chen, A. S., Djordjevic, S., Webber, J., & Gonz, A. (2020). *Investigating the Effects of Pluvial Flooding and Climate Change on Traffic Flows in Barcelona and Bristol*.

Ganin, A. A., Kitsak, M., Marchese, D., Keisler, J. M., Seager, T., & Linkov, I. (2017). Resilience and efficiency in transportation networks. *Science Advances, 3*(12), Article e1701079. https://doi.org/10.1126/sciadv.1701079

Gao, L., Liu, X., Liu, Y., Wang, P., Deng, M., Zhu, Q., & Li, H. (2019). Measuring road network topology vulnerability by Ricci curvature. *Physica A: Statistical Mechanics and Its Applications, 527*, Article 121071. https://doi.org/10.1016/j.physa.2019.121071

Geoportal of Piedmont, Administrative areas. (n.d.). Retrieved February 28, 2025, from https://www.geoportale.piemonte.it/geonetwork/srv/ita/catalog.search#/metadata/r_piemon:56e122a6-f3b1-4436-a49c-2b96dab53239.

Geoportal of Piedmont, Arpa Piemonte, Floodable areas. (n.d.). Retrieved March 3, 2025, from https://www.geoportale.piemonte.it/geonetwork/srv/ita/catalog.search#/metadata/arlpa_to:07.03.01_ai-D_2013-10-08:14:38.

Geoportal of Piedmont, Arpa Piemonte, Hydrographic basins. (n.d.). Retrieved February 28, 2025, from https://www.geoportale.piemonte.it/geonetwork/srv/ita/catalog.search#/metadata/arlpa_to:12.01.01-D_2011-06-21-11:30.

Geurs, K. T., & Van Wee, B. (2004). Accessibility evaluation of land-use and transport strategies: Review and research directions. *Journal of Transport Geography, 12*(2), 127–140. https://doi.org/10.1016/j.jtrangeo.2003.10.005

Hansen, W. G. (1959). How accessibility shapes land use. *Journal of the American Institute of Planners, 25*(2), 73–76. https://doi.org/10.1080/01944365908978307

He, H., Li, R., Pei, J., Bilodeau, J.-P., & Huang, G. (2023). Current overview of impact analysis and risk assessment of urban pluvial flood on road traffic. *Sustainable Cities and Society, 99*, Article 104993. https://doi.org/10.1016/j.scs.2023.104993

Istituto Nazionale di Statistica, Administrative areas. (n.d.). Retrieved March 16, 2025, from https://www.istat.it/notizia/confini-delle-unita-amministrative-a-fini-statistici-al-1-gennaio-2018-2/.

Istituto Nazionale di Statistica, Commuting Matrices. (n.d.). Retrieved February 28, 2025, from https://www.istat.it/non-categorizzato/matrici-di-contiguita-distanza-e-pendolarismo/.

Kim, J., Park, S., & Kim, M. (2023). Safety map: Disaster management road network for urban resilience. *Sustainable Cities and Society, 96*, Article 104650. https://doi.org/10.1016/j.scs.2023.104650

Li, Z., Yan, W., & Wang, L. (2024). Measuring mobility resilience with network-based simulations of flow dynamics under extreme events. *Transportation Research Part D: Transport and Environment, 135*, Article 104362. https://doi.org/10.1016/j.trd.2024.104362

Liu, L., Frangopol, D. M., Mondoro, A., & Yang, D. Y. (2018). Sustainability-informed bridge ranking under scour based on transportation network performance and multiattribute utility. *Journal of Bridge Engineering, 23*(10), Article 04018082. https://doi.org/10.1061/(ASCE)BE.1943-5592.0001296

Lopez, P. A., Wiessner, E., Behrisch, M., Bieker-Walz, L., Erdmann, J., Flotterod, Y.-P., Hilbrich, R., Lucken, L., Rummel, J., & Wagner, P. (2018). Microscopic traffic simulation using SUMO. In *2018 21st International Conference on Intelligent Transportation Systems (ITSC)* (pp. 2575–2582). https://doi.org/10.1109/ITSC.2018.8569938

Mandarino, A., Luino, F., Turconi, L., & Faccini, F. (2021a). Urban geomorphology of a historical city straddling the Tanaro River (Alessandria, NW Italy). *Journal of Maps, 17*(4), 29–41. https://doi.org/10.1080/17445647.2020.1746420

Mandarino, A., Luino, F., Turconi, L., & Faccini, F. (2021b). Urban geomorphology of a historical city straddling the Tanaro River (Alessandria, NW Italy). *Journal of Maps, 17*(4), 29–41. https://doi.org/10.1080/17445647.2020.1746420

Markolf, S. A., Hoehne, C., Fraser, A., Chester, M. V., & Underwood, B. S. (2019). Transportation resilience to climate change and extreme weather events – Beyond risk and robustness. *Transport Policy, 74*, 174–186. https://doi.org/10.1016/j.tranpol.2018.11.003

Martín, B., Ortega, E., Cuevas-Wizner, R., Ledda, A., & De Montis, A. (2021). Assessing road network resilience: An accessibility comparative analysis. *Transportation Research Part D: Transport and Environment, 95*, Article 102851. https://doi.org/10.1016/j.trd.2021.102851

Mattsson, L.-G., & Jenelius, E. (2015). Vulnerability and resilience of transport systems – A discussion of recent research. *Transportation Research Part A: Policy and Practice, 81*, 16–34. https://doi.org/10.1016/j.tra.2015.06.002

Mohebbi, S., Zhang, Q., Christian Wells, E., Zhao, T., Nguyen, H., Li, M., Abdel-Mottaleb, N., Uddin, S., Lu, Q., Wakhungu, M. J., Wu, Z., Zhang, Y., Tuladhar, A., & Ou, X. (2020). Cyber-physical-social interdependencies and organizational resilience: A review of water, transportation, and cyber infrastructure systems and processes. *Sustainable Cities and Society, 62*, Article 102327. https://doi.org/10.1016/j.scs.2020.102327

Morelli, A. B., & Cunha, A. (2019). *MEASURING URBAN ROAD NETWORK RESILIENCE TO EXTREME EVENTS*.

Morelli, A. B., & Cunha, A. L. (2021). Measuring urban road network vulnerability to extreme events: An application for urban floods. *Transportation Research Part D: Transport and Environment, 93*, Article 102770. https://doi.org/10.1016/j.trd.2021.102770

Papilloud, T., & Keiler, M. (2021). Vulnerability patterns of road network to extreme floods based on accessibility measures. *Transportation Research Part D: Transport and Environment, 100*, Article 103045. https://doi.org/10.1016/j.trd.2021.103045

Pregnolato, M., Ford, A., Wilkinson, S. M., & Dawson, R. J. (2017). The impact of flooding on road transport: A depth-disruption function. *Transportation Research Part D: Transport and Environment, 55*, 67–81. https://doi.org/10.1016/j.trd.2017.06.020

Pyatkova, K., Chen, A. S., Butler, D., Vojinović, Z., & Djordjević, S. (2019). Assessing the knock-on effects of flooding on road transportation. *Journal of Environmental Management, 244*, 48–60. https://doi.org/10.1016/j.jenvman.2019.05.013

Rajput, A. A., Nayak, S., Dong, S., & Mostafavi, A. (2023). Anatomy of perturbed traffic networks during urban flooding. *Sustainable Cities and Society, 97*, Article 104693. https://doi.org/10.1016/j.scs.2023.104693

Rebally, A., Valeo, C., He, J., & Saidi, S. (2021). Flood impact assessments on transportation networks: A review of methods and associated temporal and spatial scales. *Frontiers in Sustainable Cities, 3*, Article 732181. https://doi.org/10.3389/frsc.2021.732181

Serdar, M. Z., Koç, M., & Al-Ghamdi, S. G. (2022). Urban Transportation Networks Resilience: Indicators, disturbances, and assessment methods. *Sustainable Cities and Society, 76*, Article 103452. https://doi.org/10.1016/j.scs.2021.103452

Shahdani, F. J., Santamaria-Ariza, M., Sousa, H. S., Coelho, M., & Matos, J. C. (2022). Assessing flood indirect impacts on road transport networks applying mesoscopic traffic modelling: The case Study of Santarém, Portugal. *Applied Sciences, 12*(6), 3076. https://doi.org/10.3390/app12063076

Tang, Z., Wang, P., Li, Y., Chen, C., Lou, Y., & Hu, T. (2025). Contributions of urbanization and population growth to changes in urban flood exposure in recent decades. *Sustainable Cities and Society, 130*, Article 106592. https://doi.org/10.1016/j.scs.2025.106592

Taylor, M. A. P., Sekhar, S. V. C., & D'Este, G. M. (2006). Application of accessibility based methods for vulnerability analysis of Strategic road networks. *Networks and Spatial Economics, 6*(3). https://doi.org/10.1007/s11067-006-9284-9. Article 3.

Taylor, M. (2017). *Vulnerability analysis for transportation networks—1st edition*. Elsevier. https://shop.elsevier.com/books/vulnerability-analysis-for-transportation-networks/taylor/978-0-12-811010-2.

Tom tom, Move. (n.d.). Retrieved July 22, 2025, from https://move.tomtom.com/.

Viegas, J. M., Martinez, L. M., & Silva, E. A. (2009). Effects of the modifiable areal unit problem on the delineation of traffic analysis zones. *Environment and Planning B: Planning and Design, 36*(4), 625–643. https://doi.org/10.1068/b34033

Westrum, R. (2006). A typology of resilience situations. *Resilience Engineering: Concepts and Precepts*, 55–65.

Zhang, X., Miller-Hooks, E., & Denny, K. (2015). Assessing the role of network topology in transportation network resilience. *Journal of Transport Geography, 46*, 35–45. https://doi.org/10.1016/j.jtrangeo.2015.05.006

Zhang, Y., Zhao, H., Wang, K., Lıang, J., Qıu, H., & Kou, L. (2024). Spatiotemporal assessment of post-earthquake road network resilience using a data-driven approach. *Sustainable Cities and Society, 113*, Article 105675. https://doi.org/10.1016/j.scs.2024.105675

Zhao, L., Wang, S., Wei, J., & Chen, R. (2022). Impacts of land use on urban road network vulnerability. *Journal of Urban Planning and Development, 148*(3), Article 04022032. https://doi.org/10.1061/(ASCE)UP.1943-5444.0000862

Zhou, Y., Fu, X., Tang, T., Vo, K. D., & Hato, E. (2025). Assessing resilience of transit networks: An activity-based space-time accessibility analysis. *Sustainable Cities and Society*.